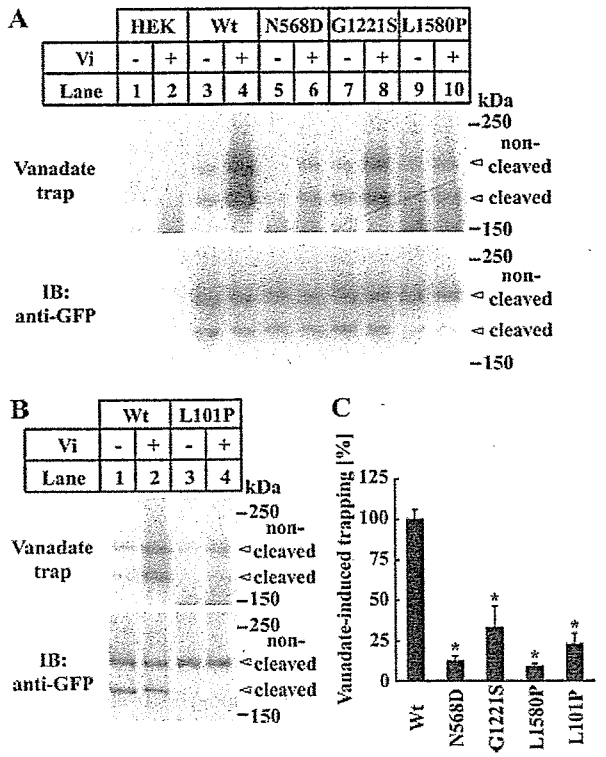

FIGURE 4. **Vanadate-induced nucleotide trapping in ABCA3-GFP and mutant proteins.** *A*, 20,000 × *g* membrane fraction prepared from HEK293 cells stably expressing the wild-type (*Wt*) ABCA3-GFP (*lanes 3* and *4*), N568D (*lanes 5* and *6*), G1221S (*lanes 7* and *8*), L1580P (*lanes 9* and *10*), or untransfected HEK293 cells (*lanes 1* and *2*) was incubated with 10 μM 8-azido-[α-^{32}P]ATP in the absence (−) or presence (+) of 0.4 mM orthovanadate (*Vi*) and 3 mM $MgCl_2$ for 10 min at 37 °C. Proteins were photoaffinity-labeled with UV irradiation after removal of unbound ATP, electrophoresed on SDS-PAGE (5%), and transferred to a PVDF membrane. Membrane was analyzed by autoradiography (*upper panel*) and immunoblotting (*IB*) using anti-GFP antibody (*lower panel*). *B*, 20,000 × *g* membrane fraction prepared from HEK293 cells stably expressing the wild-type (*Wt*) ABCA3-GFP (*lanes 1* and *2*) or L101P (*lanes 3* and *4*) was similarly analyzed. *C*, radioactivities of photoaffinity-labeled protein (total 220-kDa noncleaved form plus 180-kDa cleaved form) were quantified by FLA-5000. Radioactivities in the absence of orthovanadate were subtracted from radioactivities in the presence of orthovanadate and are expressed after normalization to ABCA3-GFP protein (total 220-kDa noncleaved form plus 180-kDa cleaved form). Data are represented as means ± S.D. ($n = 4$). *, $p < 0.005$ *versus* wild type.

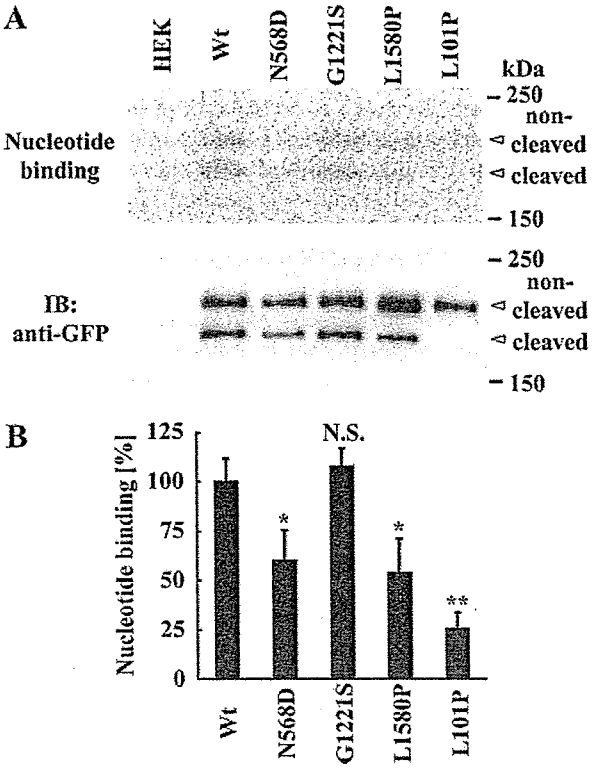

FIGURE 5. **Binding of ABCA3-GFP and mutant proteins with 8-azido-[γ-^{32}P]ATP.** *A*, 20,000 × *g* membrane fraction prepared from HEK293 cells stably expressing wild-type (*Wt*) ABCA3-GFP, N568D, G1221S, L101P, or untransfected HEK293 cells was incubated with 20 μM 8-azido-[γ-^{32}P]ATP and 3 mM $MgCl_2$ for 10 min at 0 °C. Proteins were photoaffinity-labeled with UV irradiation, immunoprecipitated using anti-human ABCA3 antibody, electrophoresed on SDS-PAGE (5%), and transferred to a PVDF membrane. Membrane was analyzed by BAS-2000 (*upper panel*) and immunoblotting (*IB*) using anti-GFP antibody (*lower panel*). *B*, radioactivities of photoaffinity-labeled protein (total 220-kDa noncleaved form plus 180-kDa cleaved form) were quantified by BAS-2000 and expressed after normalization to ABCA3-GFP protein (total 220-kDa noncleaved form plus 180-kDa cleaved form). Data are represented as means ± S.D. ($n = 3$). *, $p < 0.05$; **, $p < 0.01$ *versus* wild type. *N.S.*, not significant.

expressing wild-type or mutant (N568D, G1221S, and L1580P) ABCA3-GFP fusion proteins were established. In the stably expressing cells, wild-type and the mutant ABCA3-GFP proteins were mainly localized to intracellular vesicle membrane as in transiently expressed cells (data not shown). Among 20,000 × *g* membrane fractions of the cells expressing wild-type ABCA3-GFP, 220-kDa (noncleaved form) and 180-kDa (cleaved form) proteins were slightly photoaffinity-labeled with 8-azido-[α-^{32}P]ATP in the absence of orthovanadate (Fig. 4*A*, *lane 3*), and photoaffinity labeling was induced in the presence of orthovanadate (Fig. 4*A*, *lane 4*). Although we used ABCA3-GFP fusion protein in this study, these results are consistent with our previous observation using ABCA3 without GFP fusion (26). In the N568D, G1221S, and L1580P mutant proteins, vanadate-induced nucleotide trapping was significantly decreased to 12, 33, and 9% of that of the wild-type protein, respectively (Fig. 4, *A*, *lanes 5–10*, and *C*). These results indicate that ATP hydrolysis activity is severely impaired in these mutants.

To examine ATP hydrolysis of the mutant retained to the ER, cells stably expressing L101P mutant protein were established. L101P mutant protein was mainly localized to the ER, consistent with the result in transiently expressing cells (data not shown). The vanadate-induced nucleotide trapping also was significantly decreased compared with that of wild-type protein (Fig. 4*B*, *lanes 3* and *4*), indicating that ATP hydrolysis activity as well as intracellular trafficking is impaired in the L101P mutant protein.

ATP Binding of ABCA3-GFP and Mutants—To clarify the mechanism of loss of ATP hydrolysis activity of the N568D, G1221S, and L1580P mutant proteins, we examined ATP binding of wild-type ABCA3-GFP and the mutant proteins. Among the 20,000 × *g* membrane fractions of the cells expressing wild-type ABCA3-GFP, the 220-kDa (noncleaved form) and the 180-kDa (cleaved form) proteins were photoaffinity-labeled with 8-azido-[γ-^{32}P]ATP (Fig. 5*A*). The membrane fraction of the untransfected HEK293 cells was not photoaffinity-labeled. The level of photoaffinity labeling of the G1221S mutant protein

with 8-azido-[γ-^{32}P]ATP was similar to that of wild-type ABCA3-GFP protein (Fig. 5, *A* and *B*). However, the levels of photoaffinity labeling of N568D and L1580P mutant proteins were moderately decreased to 60 and 54% of that of wild-type protein, respectively. The level of photoaffinity labeling of L101P protein remaining localized at the ER was considerably decreased to 25% that of wild-type protein. These results suggest that decreased ATP binding contributes to impaired ATP hydrolysis in the N568D, L1580P, and L101P mutants but not in the G1221S mutant.

ATP Hydrolysis of Site-directed Mutants of Gly-1221 in 11th Transmembrane Segment—Since transmembrane domains and NBDs are suggested to communicate during the ATP hydrolysis cycle (31), local environmental changes in the 11th transmembrane segment (TM-11) resulting from the G1221S mutation might allosterically impair ATP hydrolysis activity of the ABCA3 protein. To address this, the effects of introducing hydroxyl groups or alteration of side-chain size on ATP hydrolysis activity were investigated by generating three site-directed mutants (G1221A, G1221V, and G1221T), which were stably expressed in HEK293 cells. These mutant proteins were mainly localized to intracellular vesicle membrane (data not shown). In the G1221T mutant protein, which had hydroxyl-containing amino acids, vanadate-induced nucleotide trapping was decreased to 36% of that of wild-type protein, as also in G1221S mutant protein (Fig. 6, *A*, *lanes 9–12*, and *B*). In the G1221A and G1221V mutant proteins, which have a hydrophobic side chain, vanadate-induced nucleotide trapping was decreased to 15 and 18% of that of wild-type protein, respectively (Fig. 6, *A*, *lanes 5–8*, and *B*). This result indicates the significance of the small side chain of Gly-1221 (H atom) in TM-11 for ATP hydrolysis.

ATP Hydrolysis of Site-directed Mutants of Leu-1580 in NBD-2—Because both leucine and proline are hydrophobic amino acids, alteration of side-chain size could be responsible for the impaired ATP hydrolysis in the L1580P mutant. Accordingly, Leu-1580 was substituted with three hydrophobic amino acids, Ala, Val, and Phe, of different size. All three mutant proteins were stably expressed in HEK293 cells and were mainly localized to intracellular vesicle membrane (data not shown). Substitution with Val, the side chain of which is smaller than that of Leu, resulted in decreased vanadate-induced nucleotide trapping of 56% that of wild-type protein (Fig. 7, *A*, *lanes 7* and *8*, and *B*). Substitution with Ala, the side chain of which is much smaller than that of Val, resulted in decreased vanadate-induced nucleotide trapping of 13% that of wild-type protein (Fig. 7, *A*, *lanes 5* and *6*, and *B*). On the other hand, substitution with Phe, the side chain of which is larger than that of Leu, also caused a dramatic decrease in vanadate-induced nucleotide trapping to 13% that of wild-type protein (Fig. 7, *A*, *lanes 9* and *10*, and *B*). These results indicate that appropriate side-chain size of Leu-1580 at NBD-2 is important for ATP hydrolysis of ABCA3.

Homology Modeling of NBD-2 of ABCA3—The relationship between side-chain size and ATP hydrolysis activity of Leu-1580 mutant proteins suggests side-chain contact of Leu-1580 with other amino acids in the ABCA3 protein. To address this question, the secondary structures of NBD of ABCA3 and other

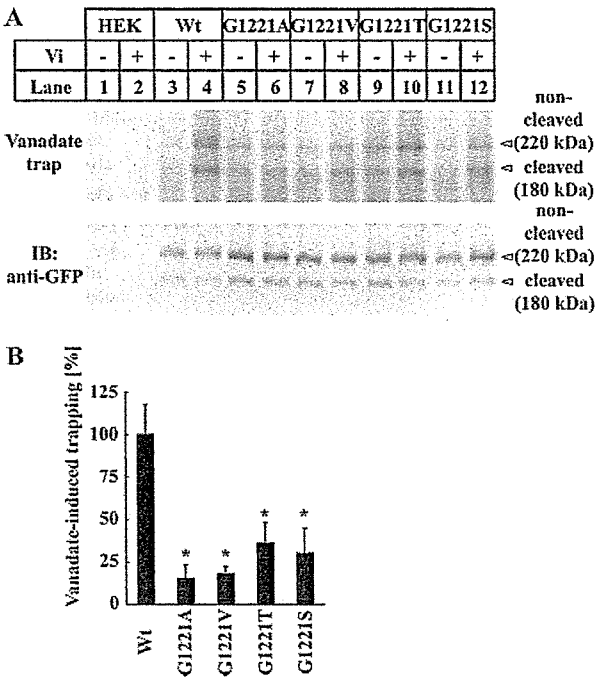

FIGURE 6. **Vanadate-induced nucleotide trapping in site-directed mutant proteins of Gly-1221.** *A*, 20,000 × *g* membrane fraction prepared from HEK293 cells stably expressing wild-type (*Wt*) ABCA3-GFP (*lanes 3* and *4*), G1221A (*lanes 5* and *6*), G1221V (*lanes 7* and *8*), G1221T (*lanes 9* and *10*), G1221S (*lanes 11* and *12*), or untransfected HEK293 cells (*lanes 1* and *2*) was incubated with 10 μM 8-azido-[α-^{32}P]ATP in the absence (−) or presence (+) of 0.4 mM orthovanadate (*Vi*) and 3 mM $MgCl_2$ for 10 min at 37 °C. Proteins were photoaffinity-labeled with UV irradiation after removal of unbound ATP, electrophoresed on SDS-PAGE (5%), and transferred to a PVDF membrane. Membrane was analyzed by autoradiography (*upper panel*) and immunoblotting (*IB*) using anti-GFP antibody (*lower panel*). *B*, radioactivities of photoaffinity-labeled protein (total 220-kDa noncleaved form plus 180-kDa cleaved form) were quantified by FLA-5000. Radioactivities in the absence of orthovanadate were subtracted from radioactivities in the presence of orthovanadate and are expressed after normalization to ABCA3-GFP protein (total 220-kDa noncleaved form plus 180-kDa cleaved form). Data are represented as means ± S.D. (n = 4–5). *, $p < 0.01$ *versus* wild type.

ABC transporters were first predicted (32) and compared with that of *Escherichia coli* maltose transporter MalK (Fig. 8*A*), of which the crystal structure has been solved (33). Leu-1580 was predicted to locate at helix 7 (referred from the study of vitamin B transporter BtuD; Ref. 34) adjacent to the H-loop His residue, which is well conserved and known to form a strong hydrogen bond with the γ-phosphate of ATP. We then modeled the structure of NBD-2 of ABCA3 based on the ATP-bound closed form of MalK (Protein Data Bank entry 1Q12; Ref. 33) using SWISS-MODEL (35). In the model of ABCA3, the orientations of His-1572 and Leu-1580 in ABCA3 were similar to those of His-192 and Leu-200 in MalK, respectively (Fig. 8, *B* and *C*). In the model of ABCA3, Trp-1554 is the most proximal residue from Leu-1580 in amino acids located at helix 6, and the distance from δ-carbon of Leu-1580 to β-carbon of Trp-1554 (the nearest carbon) was ~4.4 Å, which is close to van der Waals contact. In MalK, the distance from δ-carbon of Leu-200 to β-carbon of corresponding Arg-173 at helix 6 was ~4.2 Å, comparable with the calculated distance in ABCA3. Substitution of Leu-1580 with Pro, considering the best rotamer conformation, extended the distance from γ-carbon of Pro-1580 to β-carbon of Trp-1554 to 5.4 Å (Fig. 8*D*). In the L1580V mutant protein,

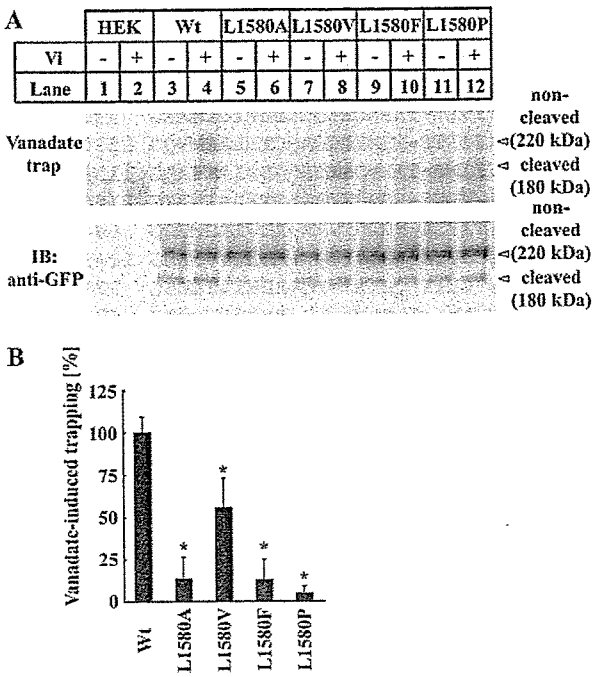

FIGURE 7. **Vanadate-induced nucleotide trapping in site-directed mutant proteins of Leu-1580.** *A*, 20,000 × *g* membrane fraction prepared from HEK293 cells stably expressing wild-type (*Wt*) ABCA3-GFP (*lanes 3* and *4*), L1580A (*lanes 5* and *6*), L1580V (*lanes 7* and *8*), L1580F (*lanes 9* and *10*), L1580P (*lanes 11* and *12*), or untransfected HEK293 cells (*lanes 1* and *2*) was incubated with 10 μM 8-azido-[α-^{32}P]ATP in the absence (−) or presence (+) of 0.4 mM orthovanadate (*Vi*) and 3 mM $MgCl_2$ for 10 min at 37 °C. Proteins were photoaffinity-labeled with UV irradiation after removal of unbound ATP, electrophoresed on SDS-PAGE (5%), and transferred to a PVDF membrane. Membrane was analyzed by autoradiography (*upper panel*) and immunoblotting (*IB*) using anti-GFP antibody (*lower panel*). *B*, radioactivities of photoaffinity-labeled protein (total 220-kDa noncleaved form plus 180-kDa cleaved form) were quantified by FLA-5000. Radioactivities in the absence of orthovanadate were subtracted from radioactivities in the presence of orthovanadate and are expressed after normalization to ABCA3-GFP protein (total 220-kDa noncleaved form plus 180-kDa cleaved form). Data are represented as means ± S.D. ($n = 3–4$). *, $p < 0.01$ *versus* wild type.

which had moderately impaired ATP hydrolysis, the distance from γ-carbon of Val-1580 to β-carbon of Trp-1554 was calculated as 4.9 Å (Fig. 8*F*). In the L1580A and L1580F mutant proteins, which had dramatically impaired ATP hydrolysis, the distance from β-carbon of Ala-1580 and ζ-carbon of Phe-1580 was extended to 6.3 Å and shortened to 2.2 Å, respectively, compared with that of wild-type protein (Fig. 8, *E* and *G*). These biochemical and modeling analyses suggest that an appropriate distance between Trp-1554 at helix 6 and 1580th amino acid at helix 7 in NBD-2 is important for ATP hydrolysis of the ABCA3 protein. Thus, impaired ATP hydrolysis in the L1580P mutant protein may result in part from the alteration of side-chain size.

DISCUSSION

Pulmonary surfactant, composed mainly of phospholipids and specific surfactant proteins, reduces the surface tension at the alveolar air-liquid interface, thereby preventing the lungs from collapsing. However, the mechanisms of surfactant production in alveolar type II cells and secretion into the alveolar space are unknown. Recently, mutations in the *ABCA3* gene were found in newborns with fatal surfactant deficiency (12). In this study, we examined the intracellular localization and *N*-glycosylation of eight ABCA3 mutant proteins, most of the mutations found in fatal surfactant deficiency to date. In addition, we examined ATP hydrolysis and ATP binding activities of the representative mutants.

Investigating the intracellular localization and *N*-glycosylation of these ABCA3 mutant proteins in HEK293 cells, we found the missense L101P, L982P, L1553P, Q1591P, and nonsense Ins1518fs mutant proteins to be predominantly localized at the ER, with impaired processing of oligosaccharide. W1142*X* mutant ABCA3 protein, another nonsense mutant reported in fatal surfactant deficiency (12), also was predominantly localized at the ER with impaired processing of oligosaccharide (data not shown).

Some mutations of ABC transporters associated with human disease have been reported to induce intracellular mislocalization of the protein. For example, R587W and Q597R mutations of ABCA1, which are found in Tangier disease patients with high density lipoprotein deficiency, appear to be impaired in intracellular trafficking and localized predominantly to the ER (36). One amino acid (Phe-508) deletion of the cystic fibrosis transmembrane conductance regulator (CFTR) hampers trafficking of protein from the ER to the plasma membrane (37), and proper folding of the CFTR protein is thought to be essential for the coat complex II-dependent export of the protein from the ER (38). Interestingly, a single amino acid is substituted with a proline residue in the four mutant ABCA3 proteins (L101P, L982P, L1553P, and Q1591P) that are retained at the ER. As three of these mutations (L101P, L982P, and L1553P) are located in the predicted α-helical structure of the ABCA3 protein (32) and the proline residue is known to be helix breaker (39), its introduction into the ABCA3 protein might well disrupt the α-helical structure and hamper proper folding and intracellular translocation. The large C-terminal deletion of the ABCA3 protein (Ins1518fs and W1142*X*) also might hamper this process. Indeed, patients with homozygous mutations of L101P, L1553P, and W1142*X* have been reported to die of surfactant deficiency during the neonatal period, and electron microscopic study of lung tissue from patients with homozygous L1553P and W1142*X* mutations revealed smaller lamellar bodies than those in normal lung tissue (12). These observations suggest that trafficking of ABCA3 protein from the ER to the intracellular LAMP3-positive vesicle is essential not only for the function of the ABCA3 protein but also for the maturation of lamellar bodies and alveolar surfactant metabolism.

In contrast, the N568D, G1221S, and L1580P mutant proteins were localized to intracellular vesicle membrane accompanied by processing of oligosaccharide from high mannose type to complex type as found in wild-type ABCA3 protein. However, vanadate-induced nucleotide trapping analysis revealed ATP hydrolysis activity to be significantly decreased in N568D, G1221S, and L1580P mutant ABCA3 proteins compared with wild type. Thus, the mechanism of surfactant deficiency because of *ABCA3* gene mutation can be classified into two categories as follows: abnormal intracellular trafficking (type I) and decreased ATP hydrolysis activity with normal intracellular trafficking (type II). Although patients with

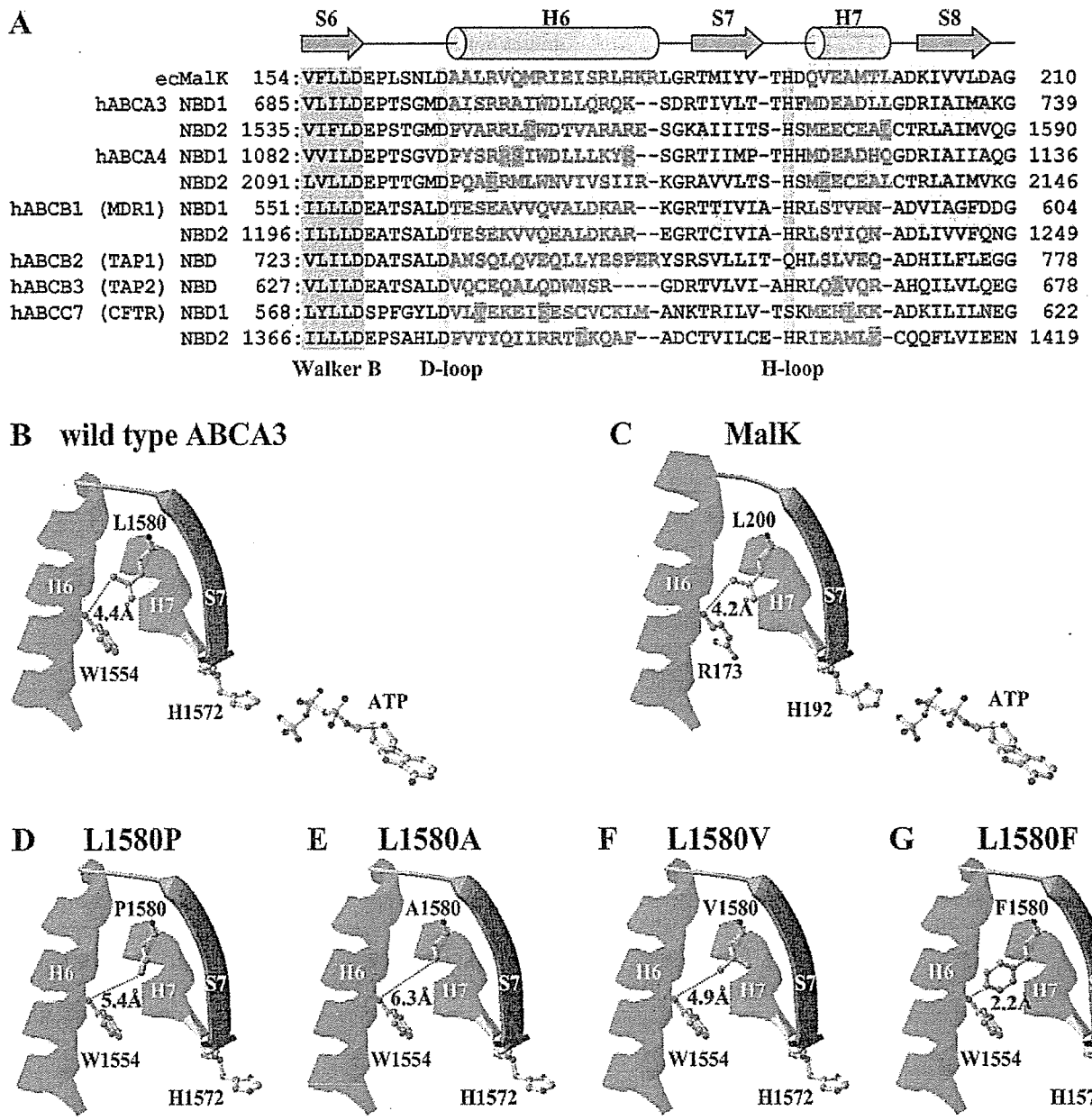

FIGURE 8. **Multiple alignment of partial NBD sequences of ABC transporters and homology modeling of NBD-2 of ABCA3.** *A*, secondary structures of NBD of human ABCA3 and other ABC transporters were predicted, and partial amino acid sequences of NBD were aligned based on the predicted secondary structures. Amino acids predicted to form α-helix, β-sheet, and coil are shown in *green*, *red*, and *black*, respectively, and compared with that of *E. coli* maltose transporter ecMalK. Critical conserved sequence motifs (Walker B, D-loop, and H-loop) are highlighted. Secondary structure elements are indicated *above* the sequence. The number of helix and sheet was referred from the study of vitamin B transporter BtuD (34). Amino acids associated with disease at helices 6 and 7 are highlighted with *yellow*. *B–G*, model structure of NBD-2 of ABCA3 (*B*) based on the ATP-bound closed form of MalK (*C*) using SWISS-MODEL is shown. For clarity, only the region from helix 6 to helix 7 is shown. The models of mutant L1580P (*D*), L1580A (*E*), L1580V (*F*), and L1580F (*G*) ABCA3 proteins were generated from that of wild-type protein by choosing the best rotamer conformation of the mutant amino acid. The 1580th residue (Leu-200 in the case of MalK) at helix 7, H-loop His residue, Trp-1554 residue (Arg-173 in the case of MalK) at helix 6, and ATP are indicated. *H*, α-helix; *S*, β-sheet.

homozygous type II *ABCA3* mutations have not been reported, patients with type I/type II compound heterozygous *ABCA3* mutations (L982P/G1221S and Ins1518fs/L1580P) died of surfactant deficiency during the neonatal period, and the lamellar bodies of lung tissue from a patient with L982P/G1221S were reported to be smaller than those from normal lung tissue (12). Because type I *ABCA3* mutation on one allele does not result in fatal surfactant deficiency, these results suggest that a sufficient level of ATP hydrolysis activity of the ABCA3 protein encoded in the other allele is essential for the function of the ABCA3 protein, maturation of the lamellar bodies, and surfactant metabolism.

Type II mutations lie in various locations as follows: N568D in the Walker A motif of NBD-1, G1221S in TM-11, and L1580P in NBD-2 (Fig. 1*A*), and all of these amino acids are conserved in the ABCA subfamily (Fig. 1, *B–D*). Because Asn-568 is highly conserved in the Walker A motif and is thought to be critical for the binding of γ-phosphate of ATP, as predicted

from the crystal structure of other ABC transporters (40), both ATP binding and ATP hydrolysis activities should be impaired in the N568D mutant protein.

It has been reported that some mutations in transmembrane domains of ABC transporters affect the activity of NBDs. For example, the E1204L mutation in TM-16 of MRP1(multidrug resistance associated protein 1) affects vanadate-induced nucleotide trapping as well as transport activity of the protein (41). In this study, mutational analysis of Gly-1221 in ABCA3 has shown the significance of the side chain of the Gly residue (H atom) in TM-11 for ATP hydrolysis. In membrane proteins, Gly is found at twice the frequency than in soluble proteins, and it is suggested that the small side chain of Gly is important for tight helix packing and helix-helix association of membrane proteins in the lipid bilayer (42). Because conserved Gly residues were found in TM-5, TM-6, TM-10, TM-11, and TM-12 of the ABCA subfamily, and also in TMs of other subfamilies such as TM-17 in the ABCC subfamily (43), these Gly residues may well contribute to the geometry of TMs that is important for communication between transmembrane domains and NBDs.

Mutational analysis of Leu-1580 suggested that impaired ATP hydrolysis in the L1580P mutant protein is in part due to the change in side-chain size. However, because Pro is known as a helix breaker (39), disruption of helix 7 by the introduction of the Pro residue may also contribute to the impaired ATP hydrolysis in the case of the L1580P mutant protein. Homology modeling of NBD-2 of ABCA3 showed that the distance between 1580th amino acid at helix 7 and Trp-1554 at helix 6 of NBD-2 is related to ATP hydrolysis of the ABCA3 protein. Because helix 7 was adjacent to the H-loop His residue, it is possible that helix 7 interacts with helix 6 to maintain the orientation of His for efficient hydrogen bonding with the γ-phosphate of ATP. Although further confirmation of this interaction might be provided by mutational analysis of Trp-1554, many disease-related mutations at helix 6 and helix 7 of NBDs such as R2106C and E2131K in ABCA4 (44–47), F587I and L610S in ABCC7/CFTR (48–50), and A665T in ABCB3/TAP2 (51) (Fig. 8*A*) support the importance of these helices for the function of the ABC transporter.

In this study, the 180-kDa cleaved protein in stably transfected cells appears to be higher in wild-type than in transiently transfected cells (Figs. 3–5). Indeed, the former is about 20–45% and the latter is about 10–20% of total 220-kDa noncleaved form plus the 180-kDa cleaved form, using total membrane fractions (data not shown). In addition, the level of vanadate-induced nucleotide trapping of the 180-kDa cleaved form protein is approximately two times higher than that of the 220-kDa noncleaved form protein after normalization to the protein level (Fig. 4*A*, *lanes 3* and *4*). Because cleaved protein is predominantly expressed in native lung tissue (21, 23), the processing of ABCA3 protein from noncleaved form to cleaved form may be physiologically important in ABCA3 function. Further studies are needed to understand the structure-function relationships of the ABCA3 protein.

We examined ATP binding and ATP hydrolysis of the type I mutant ABCA3 protein by using cells stably expressing L101P mutant protein, and we found that both ATP binding and ATP hydrolysis activities as well as intracellular trafficking were impaired in the L101P mutant protein. Although we did not examine ATP binding and ATP hydrolysis of other type I mutants, these results indicate that intracellular trafficking and also ATP binding and ATP hydrolysis activities are impaired in some type I mutant ABCA3 proteins.

Thus, intracellular trafficking and/or activity of ATP hydrolysis is dramatically impaired in the ABCA3 mutant proteins so far found in fatal surfactant deficiency patients. Such ABCA3 protein dysfunction could well underlie the severe phenotype of these patients. Very recently, it has been reported that the E292V mutation of the *ABCA3* gene is responsible in the genetic etiology of pediatric interstitial lung disease related to abnormal surfactant function (24), the phenotype of which is milder than that of fatal surfactant deficiency. It is possible that the E292V mutation causes less severe disruption of intracellular trafficking or ATP hydrolysis activity. Additional biochemical studies are required to clarify the loss of function mechanisms for the mutations associated with milder pediatric interstitial lung disease.

Very recently, Cheong *et al.* (19) reported that L101P, G1221S, and N568D mutant proteins have the most severe, moderate, and the least severe trafficking and processing defects. In this study, the difference in degree of defect between N568D and G1221S mutant proteins is slight, if any. The reason for the difference between their results and ours is unknown, but it may be due to the different clonal cells used stably expressing ABCA3 mutants. With regard to the function of the ABCA3 mutant proteins, their findings indicating impaired colocalization of fluorescence-labeled phosphatidylcholine with ABCA3-positive vesicles in G1221S and N568D may well correlate with our findings indicating impaired ATP hydrolysis activities of these mutants.

In summary, the mechanisms of surfactant deficiency because of *ABCA3* gene mutation can be classified into two categories, type I and type II, abnormal intracellular trafficking and decreased ATP hydrolysis activity. This distinction may be useful in assessing both the severity and effective therapy for lung disease because of mutation of the *ABCA3* gene.

Acknowledgments—We thank Drs. Jun-ichi Miyazaki (Osaka University) and Hitoshi Niwa (RIKEN, Kobe) for providing the pCAGIpuro plasmid.

REFERENCES

1. Rooney, S. A. (2001) *Comp. Biochem. Physiol.* **129,** 233–243
2. Mason, R. J., and Voelker, D. R. (1998) *Biochim. Biophys. Acta* **1408,** 226–240
3. Chander, A., and Fisher, A. B. (1990) *Am. J. Physiol.* **258,** L241–L253
4. Wright, J. R., and Dobbs, L. G. (1991) *Annu. Rev. Physiol.* **53,** 395–414
5. Dobbs, L. G. (1994) *Am. J. Respir. Crit. Care Med.* **150,** S31–S32
6. Batenburg, J. J., and Whitsett, J. A. (1989) *Biochim. Biophys. Acta* **1006,** 329–334
7. Zimmermann, L. J., Hogan, M., Carlson, K. S., Smith, B. T., and Post, M. (1993) *Am. J. Physiol.* **264,** L575–L580
8. Beneke, S., and Rooney, S. A. (2001) *Biochim. Biophys. Acta* **1534,** 56–63
9. Liley, H. G., White, R. T., Warr, R. G., Benson, B. J., Hawgood, S., and Ballard, P. L. (1989) *J. Clin. Investig.* **83,** 1191–1197

10. Nogee, L. M., de Mello, D. E., Dehner, L. P., and Colten, H. R. (1993) *N. Engl. J. Med.* **328,** 406–410
11. Nogee, L. M., Dunbar, A. E., III, Wert, S. E., Askin, F., Hamvas, A., and Whitsett, J. A. (2001) *N. Engl. J. Med.* **344,** 573–579
12. Shulenin, S., Nogee, L. M., Annilo, T., Wert, S. E., Whitsett, J. A., and Dean, M. (2004) *N. Engl. J. Med.* **350,** 1296–1303
13. Hawgood, S., Derrick, M., and Poulain, F. (1998) *Biochim. Biophys. Acta* **1408,** 150–160
14. Whitsett, J. A., and Weaver, T. E. (2002) *N. Engl. J. Med.* **347,** 2141–2148
15. deMello, D. E., Nogee, L. M., Heyman, S., Krous, H. F., Hussain, M., Merritt, T. A., Hsueh, W., Haas, J. E., Heidelberger, K., Schumacher, R., and Colten, H. R. (1994) *J. Pediatr.* **125,** 43–50
16. Beers, M. F., and Mulugeta, S. (2005) *Annu. Rev. Physiol.* **67,** 663–696
17. Horowitz, A. D., Baatz, J. E., and Whitsett, J. A. (1993) *Biochemistry* **32,** 9513–9523
18. Glasser, S. W., Burhans, M. S., Korfhagen, T. R., Na, C. L., Sly, P. D., Ross, G. F., Ikegami, M., and Whitsett, J. A. (2001) *Proc. Natl. Acad. Sci. U. S. A.* **98,** 6366–6371
19. Cheong, N., Madesh, M., Gonzales, L. W., Zaho, M., Yu, K., Ballard, P. L., and Shuman, H. (2006) *J. Biol. Chem.* **281,** 9791–9800
20. Thomas, A. Q., Lane, K., Phillips, J., III, Prince, M., Markin, C., Speer, M., Schwartz, D. A., Gaddipati, R., Marney, A., Johnson, J., Roberts, R., Haines, J., Stahlman, M., and Loyd, J. E. (2002) *Am. J. Respir. Crit. Care Med.* **165,** 1322–1328
21. Yamano, G., Funahashi, H., Kawanami, O., Zhao, L. X., Ban, N., Uchida, Y., Morohoshi, T., Ogawa, J., Shioda, S., and Inagaki, N. (2001) *FEBS Lett.* **508,** 221–225
22. Mulugeta, S., Gray, J. M., Notarfrancesco, K. L., Gonzales, L. W., Koval, M., Feinstein, S. I., Ballard, P. L., Fisher, A. B., and Shuman, H. (2002) *J. Biol. Chem.* **277,** 22147–22155
23. Yoshida, I., Ban, N., and Inagaki, N. (2004) *Biochem. Biophys. Res. Commun.* **323,** 547–555
24. Bullard, J. E., Wert, S. E., Whitsett, J. A., Dean, M., and Nogee, L. M. (2005) *Am. J. Respir. Crit. Care Med.* **172,** 1026–1031
25. Niwa, H., Yamamura, K., and Miyazaki, J. (1991) *Gene (Amst.)* **108,** 193–199
26. Nagata, K., Yamamoto, A., Ban, N., Tanaka, A. R., Matsuo, M., Kioka, N., Inagaki, N., and Ueda, K. (2004) *Biochem. Biophys. Res. Commun.* **324,** 262–268
27. Matsuo, M., Kioka, N., Amachi, T., and Ueda, K. (1999) *J. Biol. Chem.* **274,** 37479–37482
28. Matsuo, M., Tanabe, K., Kioka, N., Amachi, T., and Ueda, K. (2000) *J. Biol. Chem.* **275,** 28757–28763
29. Voorhout, W. F., Veenendaal, T., Haagsman, H. P., Weaver, T. E., Whitsett, J. A., van Golde, L. M., and Geuze, H. J. (1992) *Am. J. Physiol.* **263,** L479–L486
30. Wang, W. J., Russo, S. J., Mulugeta, S., and Beers, M. F. (2002) *J. Biol. Chem.* **277,** 19929–19937
31. Higgins, C. F., and Linton, K. J. (2004) *Nat. Struct. Mol. Biol.* **11,** 918–926
32. McGuffin, L. J., Bryson, K., and Jones, D. T. (2000) *Bioinformatics (Oxf.)* **16,** 404–405
33. Chen, J., Lu, G., Lin, J., Davidson, A. L., and Quiocho, F. A. (2003) *Mol. Cell* **12,** 651–661
34. Locher, K. P., Lee, A. T., and Rees, D. C. (2002) *Science* **296,** 1091–1098
35. Schwede, T., Kopp, J., Guex, N., and Peitsch, M. C. (2003) *Nucleic Acids Res.* **31,** 3381–3385
36. Tanaka, A. R., Abe-Dohmae, S., Ohnishi, T., Aoki, R., Morinaga, G., Okuhira, K., Ikeda, Y., Kano, F., Matsuo, M., Kioka, N., Amachi, T., Murata, M., Yokoyama, S., and Ueda, K. (2003) *J. Biol. Chem.* **278,** 8815–8819
37. Jensen, T. J., Loo, M. A., Pind, S., Williams, D. B., Goldberg, A. L., and Riordan, J. R. (1995) *Cell* **83,** 129–135
38. Wang, X., Matteson, J., An, Y., Moyer, B., Yoo, J. S., Bannykh, S., Wilson, I. A., Riordan, J. R., and Balch, W. E. (2004) *J. Cell Biol.* **167,** 65–74
39. Prevelige, P., Jr., and Fasman, G. (1989) in *Prediction of Protein Structure and the Principles of Protein Conformation* (Fasman, G., ed) pp. 391–416, Plenum Publishing Corp., New York
40. Davidson, A. L., and Chen, J. (2004) *Annu. Rev. Biochem.* **73,** 241–268
41. Situ, D., Haimeur, A., Conseil, G., Sparks, K. E., Zhang, D., Deeley, R. G., and Cole, S. P. (2004) *J. Biol. Chem.* **279,** 38871–38880
42. Eilers, M., Shekar, S. C., Shieh, T., Smith, S. O., and Fleming, P. J. (2000) *Proc. Natl. Acad. Sci. U. S. A.* **97,** 5796–5801
43. Zhang, D. W., Gu, H. M., Vasa, M., Muredda, M., Cole, S. P., and Deeley, R. G. (2003) *Biochemistry* **42,** 9989–10000
44. Rivera, A., White, K., Stohr, H., Steiner, K., Hemmrich, N., Grimm, T., Jurklies, B., Lorenz, B., Scholl, H. P., Apfelstedt-Sylla, E., and Weber, B. H. (2002) *Am. J. Hum. Genet.* **67,** 800–813
45. Fumagalli, A., Ferrari, M., Soriani, N., Gessi, A., Foglieni, B., Martina, E., Manitto, M. P., Brancato, R., Dean, M., Allikmets, R., and Cremonesi, L. (2001) *Hum. Genet.* **109,** 326–338
46. Allikmets, R., Singh, N., Sun, H., Shroyer, N. F., Hutchinson, A., Chidambaram, A., Gerrard, B., Baird, L., Stauffer, D., Peiffer, A., Rattner, A., Smallwood, P., Li, Y., Anderson, K. L., Lewis, R. A., Nathans, J., Leppert, M., Dean, M., and Lupski, J. R. (1997) *Nat. Genet.* **15,** 236–246
47. Lewis, R. A., Shroyer, N. F., Singh, N., Allikmets, R., Hutchinson, A., Li, Y., Lupski, J. R., Leppert, M., and Dean, M. (1999) *Am. J. Hum. Genet.* **64,** 422–434
48. des Georges, M., Guittard, C., Altieri, J. P., Templin, C., Sarles, J., Sarda, P., and Claustres, M. (2004) *J. Cyst. Fibros.* **3,** 265–272
49. Vankeerberghen, A., Wei, L., Jaspers, M., Cassiman, J. J., Nilius, B., and Cuppens, H. (1998) *Hum. Mol. Genet.* **7,** 1761–1769
50. Dork, T., Dworniczak, B., Aulehla-Scholz, C., Wieczorek, D., Bohm, I., Mayerova, A., Seydewitz, H. H., Nieschlag, E., Meschede, D., Horst, J., Pander, H. J., Sperling, H., Ratjen, F., Passarge, E., Schmidtke, J., and Stuhrmann, M. (1997) *Hum. Genet.* **100,** 365–377
51. Colonna, M., Bresnahan, M., Bahram, S., Strominger, J. L., and Spies, T. (1992) *Proc. Natl. Acad. Sci. U. S. A.* **89,** 3932–3936

A T3587G germ-line mutation of the *MDR1* gene encodes a nonfunctional P-glycoprotein

Kazuyoshi Mutoh,[1] Junko Mitsuhashi,[1,2] Yasuhisa Kimura,[7] Satomi Tsukahara,[2] Etsuko Ishikawa,[2] Kimie Sai,[3,4] Shogo Ozawa,[3,5] Jun-ichi Sawada,[3,6] Kazumitsu Ueda,[7] Kazuhiro Katayama,[1] and Yoshikazu Sugimoto[1,2]

[1]Department of Chemotherapy, Kyoritsu University of Pharmacy; [2]Division of Gene Therapy, Cancer Chemotherapy Center, Japanese Foundation for Cancer Research; [3]Project Team for Pharmacogenetics and Divisions of [4]Xenobiotic Metabolism and Disposition, [5]Pharmacology, and [6]Biochemistry and Immunochemistry, National Institute of Health Sciences, Tokyo, Japan and [7]Laboratory of Biochemistry, Division of Applied Life Sciences, Graduate School of Agriculture, Kyoto University, Kyoto, Japan

Abstract

The human *multidrug resistance gene 1* (*MDR1*) encodes a plasma membrane P-glycoprotein (P-gp) that functions as an efflux pump for various structurally unrelated anticancer agents. We have identified two nonsynonymous germ-line mutations of the *MDR1* gene, C3583T *MDR1* and T3587G *MDR1*, in peripheral blood cell samples from Japanese cancer patients. Two patients carried the C3583T *MDR1* allele that encodes H1195Y P-gp, whereas a further two carried T3587G *MDR1* that encodes I1196S P-gp. Murine NIH3T3 cells were transfected with pCAL-MDR-IRES-ZEO constructs carrying either wild-type (WT), C3583T, or T3587G *MDR1* cDNA and selected with zeocin. The resulting zeocin-resistant mixed populations of transfected cells were designated as 3T3/WT, 3T3/H1195Y, and 3T3/I1196S, respectively. The cell surface expression of I1196S P-gp in 3T3/I1196S cells could not be detected by fluorescence-activated cell sorting, although low expression of I1196S P-gp was found by Western blotting. H1195Y P-gp expression levels in 3T3/H1195Y cells were slightly lower than the corresponding WT P-gp levels in 3T3/WT cells. By immunoblotting analysis, both WT P-gp and H1195Y P-gp were detectable as a 145-kDa protein, whereas I1196S P-gp was visualized as a 140-kDa protein. 3T3/I1196S cells did not show any drug resistance unlike 3T3/H1195Y cells. Moreover, a vanadate-trap assay showed that the I1196S P-gp species lacks ATP-binding activity. Taken together, we conclude from these data that T3587G *MDR1* expresses a nonfunctional P-gp and this is therefore the first description of such a germ-line mutation. We contend that the T3587G *MDR1* mutation may affect the pharmacokinetics of *MDR1*-related anticancer agents in patients carrying this allele. [Mol Cancer Ther 2006; 5(4):877–84]

Introduction

P-glycoprotein (P-gp), also known as ABCB1, is a 170- to 180-kDa transmembrane glycoprotein that functions as an efflux pump for various structurally unrelated anticancer drugs, such as the *Vinca* alkaloids, anthracyclines, and taxanes (1–4). P-gp is expressed in a variety of normal human tissues and cells, such as the small and large intestine, adrenal gland, kidney, liver, placenta, and the capillary endothelial cells of the brain and testes (5, 6). P-gp also mediates the excretion of its substrates from the intestine and therefore inhibits their intestinal absorption (7). In addition, P-gp mediates the biliary excretion and renal tubular secretion of its substrates (8, 9). Moreover, the coadministration of P-gp substrate anticancer agents and P-gp inhibitors, such as verapamil, increases both the plasma concentration and the area under the concentration-time curve of these substrate agents (10, 11). Mice lacking *multidrug resistance gene 1* (*MDR1*)-type P-gps (*mdr1a/mdr1b−/−* mice) display large changes in the pharmacokinetics of digoxin and other drugs (12, 13). Hence, the low expression of P-gp in normal cells/tissues alters the pharmacokinetics of its substrate anticancer agents.

Recently, single nucleotide polymorphisms (SNP) have been extensively investigated, as several of them have been shown to alter mRNA and/or protein expression levels. As P-gp determines the pharmacokinetics of several anticancer drugs, *MDR1* SNPs that affect P-gp expression and function have been of particular interest. A synonymous SNP in the *MDR1* gene, C3435T, which does not cause an amino acid substitution, was reported to be associated with low intestinal P-gp expression, low P-gp activity, and high digoxin absorption in individuals carrying this allele (14–16). Furthermore, our haplotype analysis has now further revealed that a *MDR1**2 haplotype with a linkage of C1236T *MDR1* (synonymous), G2677T *MDR1* (A893S P-gp), and C3435T *MDR1* is associated with a reduced renal excretion of irinotecan in Japanese cancer patients possibly due to a reduced P-gp function (17). However, the molecular mechanisms underlying the low renal excretion of irinotecan in this instance are still unclear.

Received 7/12/05; revised 12/25/05; accepted 1/25/06.

Grant support: Ministry of Education, Culture, Sports, Science and Technology and Ministry of Health, Labor and Welfare, Japan.

The costs of publication of this article were defrayed in part by the payment of page charges. This article must therefore be hereby marked advertisement in accordance with 18 U.S.C. Section 1734 solely to indicate this fact.

Requests for reprints: Yoshikazu Sugimoto, Department of Chemotherapy, Kyoritsu University of Pharmacy, 1-5-30 Shibakoen, Minato-ku, Tokyo 105-8512, Japan. Phone: 81-3-5400-2670; Fax: 81-3-5400-2669. E-mail: sugimoto-ys@kyoritsu-ph.ac.jp

doi:10.1158/1535-7163.MCT-05-0240

We have also reported previously the identification of a T3587G *MDR1* germ-line mutation in a Japanese patient, which confers a serine substitution for Ile^{1196} in P-gp (I1196S P-gp; ref. 17). We subsequently attempted to evaluate the possible functional alterations that may be caused by this substitution by analyzing the renal clearance of irinotecan in this individual who was heterozygous for the T3587G *MDR1*. There was an indication that the T3587G *MDR1* may be associated with high renal clearance of SN-38, but this observation was too preliminary to draw any firm conclusions as only one heterozygous patient was analyzed. This finding, however, prompted us to functionally characterize the Ser^{1196} substitution using *MDR1* cDNA-transfected cells and to further analyze additional Japanese subjects for the presence of other *MDR1* SNPs. We were subsequently able to identify a novel germ-line mutation in the *MDR1* gene, C3583T *MDR1*, which causes a substitution of tyrosine for His^{1195} in the P-gp (H1195Y P-gp). In our current study, we have established T3587G *MDR1* and C3583T *MDR1* cDNA transfectants and examined both expression levels and functional properties of I1196S P-gp and H1195Y P-gp. Our findings show that the T3587G *MDR1* cDNA encodes a nonfunctional P-gp and that the C3583T *MDR1* cDNA encodes a functional P-gp.

Materials and Methods

Sequence Analysis of the *MDR1* Gene

Peripheral blood nucleated cells were obtained from both healthy volunteers and cancer patients of Japanese nationality, after obtaining written informed consent, to undertake genetic analysis from each of these individuals. Exon 27 of the *MDR1* gene, which incorporates nucleotides 3,490 to 3,636 from the first ATG codon of the mRNA, was amplified by PCR from genomic DNA samples using the forward and reverse primers: 5′-CTTTACTTTCAGTTCTACTTTCA-3′ and 5′-GAGAATACAGCATTTTTAAGGA-3′, respectively. The resulting PCR products were directly sequenced using the primer 5′-CAGTTCTACTTTCATAACAACA-3′.

MDR1 Vectors

For the transfection of *MDR1* cDNA, we generated pCAL-MDR-IRES-ZEO bicistronic constructs, in which either wild-type (WT) or mutant *MDR1* cDNA insert was cloned upstream of the internal ribosome entry site (IRES) of the encephalomyocarditis virus. In the resulting transfectants, a single bicistronic mRNA species is transcribed under the control of the CAG promoter consisting of a cytomegalovirus immediate-early enhancer, a chicken β-actin transcription start site, and a rabbit β-globin intron (18). The upstream *MDR1* cDNA is translated in a cap-dependent manner, and the downstream *zeocin resistance gene* (*ZEO*) is translated under the control of the IRES.

For the retrovirus-mediated transfer of *MDR1* cDNAs, we constructed pHa-MDR-IRES-DHFR bicistronic retroviral vector plasmids, in which either WT or mutant *MDR1* cDNA insert was cloned upstream of the IRES.

Establishment of Mutant *MDR1* Transfectants

Murine fibroblast NIH3T3 cells were cultured in DMEM supplemented with 7% fetal bovine serum at 37°C in a humidified 5% CO_2 environment. For the establishment of WT or mutant *MDR1* transfectants, NIH3T3 cells were transfected with pCAL-MDR-IRES-ZEO containing either WT *MDR1*, C3583T *MDR1*, or T3587G *MDR1* cDNA. The cells were selected with 50 μg/mL zeocin and the resulting zeocin-resistant colonies were mixed. The zeocin-resistant mixed populations of the transfected cells were designated as 3T3/WT, 3T3/H1195Y, and 3T3/I1196S, respectively. Because 3T3/I1196S cells expressed only a small amount of P-gp, we isolated 30 T3587G *MDR1* cDNA transfectant clones by limiting dilution and tested for P-gp expression. A clone with the highest I1196S P-gp expression, designated as 3T3/I1196S clone 23, was used in the evaluation of ATP-binding activity of mutant P-gps.

The anticancer agent resistance levels in parental NIH3T3 cells and in the various *MDR1* transfectants were evaluated by cell growth inhibition assays after incubation of the cells for 5 days at 37°C in the absence or presence of various concentrations of vincristine or doxorubicin. Cell numbers were determined with a cell counter (Sysmex, Kobe, Japan).

Retrovirus-Mediated Mutant *MDR1* Gene Transfer

For retrovirus-mediated transfer of *MDR1* cDNAs, PA317 amphotropic retrovirus packaging cells were transfected with the pHa-MDR-IRES-DHFR plasmid containing either WT *MDR1*, C3583T *MDR1*, or T3587G *MDR1* cDNA insert using a calcium phosphate coprecipitation method. The transfectants were then selected by exposure to 120 ng/mL methotrexate and Ha-MDR-IRES-DHFR retrovirus-containing supernatants were harvested. NIH3T3 cells were then transduced with each of the Ha-MDR-IRES-DHFR retrovirus preparations following centrifugation at 2,800 rpm for 2 hours in the presence of polybrene (6 μg/mL) and cultured further in medium without retrovirus.

Fluorescence-Activated Cell Sorting Analysis of P-gp Expression

The expression levels of human P-gp on the cell surfaces of various *MDR1* transfectants were examined by fluorescence-activated cell sorting (FACS) analysis using a human-specific monoclonal antibody MRK16, which reacts with a cell surface epitope of P-gp. The cells were incubated with or without a biotinylated $F(ab')_2$ fragment of MRK16 (100 μg/mL) followed by washing and incubation with R-phycoerythrin-conjugated streptavidin (400 μg/mL; BD Biosciences, Franklin Lakes, NJ; ref. 19). Fluorescence staining levels were measured using FACSCalibur (BD Biosciences).

Western Blotting

Cell lysates of the *MDR1* transfectants were separated by SDS-PAGE and then electrotransferred onto a nitrocellulose membrane. The membrane was incubated with 1 μg/mL anti-P-gp monoclonal antibody C219 (Cencor, Malvern, PA; ref. 20) followed by washing and treatment with peroxidase-conjugated sheep anti-mouse secondary antibody (Amersham, Buckinghamshire, United Kingdom). The membrane-bound antibody was visualized with Enhanced Chemiluminescence Plus Detection kit (Amersham).

Genomic PCR and Reverse Transcription-PCR

Genomic DNA was extracted from each of the transfectants with a DNeasy Tissue kit (Qiagen, Valencia, CA) according to the manufacturer's instructions. *MDR1* cDNA (3,561 bp) was then amplified by PCR using the forward and reverse primers, 5′-CACGTGGTTGGAAGCTAACC-3′ and 5′-GAAGGCCAGAGCATAAGATGC-3′, respectively. As an internal control, the *glyceraldehyde-3-phosphate dehydrogenase* (*GAPDH*) gene (551-bp fragment) was amplified with the forward and reverse primers, 5′-ATCACCATCTTCCAGGAGCGA-3′ and 5′-GCTTCACCACCTTCTTGATGT-3′, respectively. The PCR conditions for *MDR1* amplification were as follows: 95°C for 5 minutes followed by 35 cycles of 95°C for 1 minute, 55°C for 1 minute, and 72°C for 3 minutes and a final extension at 72°C for 7 minutes. The *GAPDH* control amplification conditions were as follows: 95°C for 5 minutes followed by 20 cycles of 95°C for 30 seconds, 55°C for 30 seconds, and 72°C for 1 minute and a final extension at 72°C for 7 minutes.

The isolation of total RNA and subsequent reverse transcription-PCR was done using a RNeasy kit (Qiagen) and a RNA LA PCR kit (Takara, Ohtsu, Japan), each according to the manufacturer's instructions. First-strand *MDR1* cDNA was synthesized from 0.3 μg total RNA and a 702-bp *MDR1* cDNA fragment was amplified by PCR with the forward and reverse primers, 5′-GATATCAATGATACAGGGTT-3′ and 5′-TGTCCAATAGAATATTCCCC-3′, respectively. The PCR conditions were as follows: 95°C for 5 minutes followed by 18 to 24 cycles of 95°C for 30 seconds, 55°C for 30 seconds, and 72°C for 1 minute and a final extension at 72°C for 7 minutes. As an internal control, the amplification of *GAPDH* cDNA (551-bp fragment) was carried out as described above.

Vanadate-Induced Nucleotide Trapping in P-gp with 8-Azido-[α-32P]ATP

The ATP-binding activity of P-gp was examined by vanadate-induced nucleotide trapping analysis as described previously (21). Briefly, membrane fractions (5-20 μg) were prepared from *MDR1* transfectants and incubated with 10 μL buffer containing 10 μmol/L 8-azido-[α-^{32}P]ATP, 200 μmol/L orthovanadate, 3 mmol/L $MgCl_2$, 2 mmol/L ouabain, 0.1 mmol/L EGTA, and 40 mmol/L Tris-HCl (pH 7.5) in the absence or presence of 50 μmol/L verapamil for 10 minutes at 37°C. The reactions were stopped by the addition of 500 μL ice-cold TE buffer [40 mmol/L Tris-HCl (pH 7.5), 0.1 mmol/L EGTA]. The supernatants containing unbound ATP were removed from the membrane pellet after centrifugation (15,000 × *g*, 5 minutes, 4°C), and this procedure was repeated once more. The pellets were then resuspended in 8 μL TE buffer and irradiated for 5 minutes (at 254 nm, 8.2 mW/cm^2) on ice. The samples were then electrophoresed on a 7% SDS-polyacrylamide gel, electrotransferred to polyvinylidene difluoride membranes, and analyzed by autoradiography using a radioimaging analyzer (BAS2500, Fuji Photo Film Co., Tokyo, Japan). The polyvinylidene difluoride membranes were further analyzed by Western blotting with the anti-P-gp antibody C219. The P-gp expression levels were quantified using Scion Image software (Scion, Frederick, MD). The quantities of trapped 8-azido-[α-^{32}P]ATP in the WT and mutant P-gps, expressed as RI intensities in BAS2500, were normalized to the P-gp expression levels, and the relative photoaffinity labeling of each was then plotted. Two independent experiments were done, and the average of these analyses is shown.

Results

Frequency of the C3583T *MDR1* and T3587G *MDR1*

We identified previously a germ-line mutation of the *MDR1* gene, T3587G (17), in a Japanese cancer patient who was heterozygous for this allele and have now identified another germ-line mutation of the *MDR1* gene, C3583T, in a normal Japanese population. The C3583T *MDR1* and T3587G *MDR1* alleles encode H1195Y P-gp and I1196S P-gp, respectively, and both of the His^{1195} and Ile^{1196} residues are located in the Walker B region of the second ATP-binding site of P-gp (Fig. 1A). To examine the frequencies of occurrence for these mutations, we analyzed the genomic sequences of exon 27 of the *MDR1* gene, which incorporates the nucleotide region 3,490 to 3,636 of the mRNA. Of the 605 samples that we examined, two individuals were found to be heterozygous for the C3583T allele and an additional two subjects were found to be T3587G heterozygotes. Because of their low frequencies (<1%), C3583T *MDR1* and T3587G *MDR1* germ-line mutations would therefore be called naturally occurring base changes and not SNPs. We have not thus far identified any individuals who are homozygous for either of these mutations, nor have we observed individuals who are heterozygous for a combination of the C3583T and T3587G alleles.

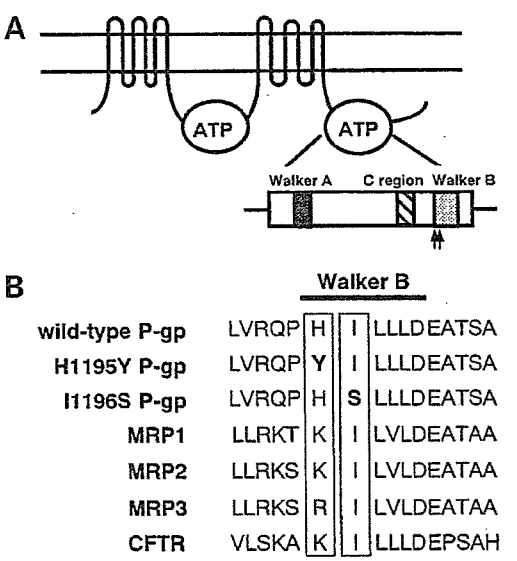

Figure 1. Map of specific mutations in P-gp. **A,** structure of P-gp. *Arrows,* location of the H1195Y and I1196S substitutions. **B,** alignment of various ATP-binding cassette transporter sequences close to the Walker B region of the second ATP-binding site. The His^{1195} and Ile^{1196} residues affected by the C3583T and T3587G mutations, together with the corresponding amino acids of other transporters, are boxed.

P-gp Expression Levels in the *MDR1* Transfectants

To investigate the molecular functions of the H1195Y mutant P-gp and I1196S mutant P-gp, we generated 3T3/WT, 3T3/H1195Y, and 3T3/I1196S cells, which were stably transfected with WT *MDR1*, C3583T *MDR1*, and T3587G *MDR1* cDNA, respectively. The P-gp expression levels on the cell surfaces of these transfectants were subsequently examined by FACS analysis using the MRK16 antibody, which recognizes a cell surface epitope of human P-gp. Both 3T3/WT and 3T3/H1195Y cells express P-gp on their cell surface, although these expression levels in 3T3/H1195Y cells (mean channel, 510) were slightly lower than in 3T3/WT cells (mean channel, 980; Fig. 2A). Surprisingly, the 3T3/I1196S cells did not express P-gp on their cell surface (Fig. 2A). We then examined the P-gp expression levels in the NIH3T3 cells and *MDR1* transfectants by Western blotting. In parental NIH3T3 cells, endogenous P-gp is expressed at very low levels (Fig. 2B). Moreover, both WT P-gp and H1195Y P-gp were detectable as a 145-kDa protein, whereas I1196S P-gp was observed as a 140-kDa protein (Fig. 2B). In addition, the expression levels of I1196S P-gp in 3T3/I1196S cells were at significantly lower levels than the other P-gp species.

As the expression levels of I1196S P-gp were very low in 3T3/I1196S cells, we examined the copy number of exogenous *MDR1* cDNA and the expression level of *MDR1* mRNA in these transfectants. A 3,561-bp human *MDR1* cDNA fragment, which is close to the full-length open reading frame, was amplified from genomic DNA isolates of the various *MDR1* cDNA transfectants. Each of the transfectants was found to have similar copy numbers of *MDR1* cDNA (Fig. 2C). We next did semiquantitative reverse transcription-PCR of *MDR1* mRNA in the transfectants. As shown in Fig. 2D, each of the *MDR1* transfectants also express similar levels of *MDR1* transcripts.

We then did retrovirus-mediated transfer of *MDR1* cDNAs to confirm the differences that we had observed in the expression levels of mutant P-gps. Amphotropic retrovirus was prepared from PA317 cells transfected with the pHa-MDR-IRES-DHFR vectors carrying either WT or mutant *MDR1* cDNA insert. NIH3T3 cells were then transduced with these *MDR1* retroviral preparations and the cells were cultured for 2 days and analyzed by FACS. As shown in Fig. 3, P-gp expression was observed in NIH3T3 cells transduced with both WT and H1195Y *MDR1* retroviruses but not in cells transduced with I1196S *MDR1* retrovirus. Transduction efficiencies were 70% and 60% for WT and H1195Y *MDR1* retroviruses, respectively. P-gp expression in cells transduced with H1195Y *MDR1* retrovirus was again found to be at a slightly lower levels than in cells transduced with WT *MDR1* retrovirus (Fig. 3B and C).

Drug Resistance in *MDR1* Transfectants

We next examined the drug resistance levels in our *MDR1* transfectants. 3T3/WT cells showed a 22-fold higher resistance to vincristine and 7-fold higher resistance to doxorubicin than parental NIH3T3 cells (Fig. 4). 3T3/H1195Y cells also showed higher levels of resistance to these drugs compared with the parental cells, but these were at slightly lower levels than 3T3/WT cells (Fig. 4). These findings correlated with the expression levels of P-gp

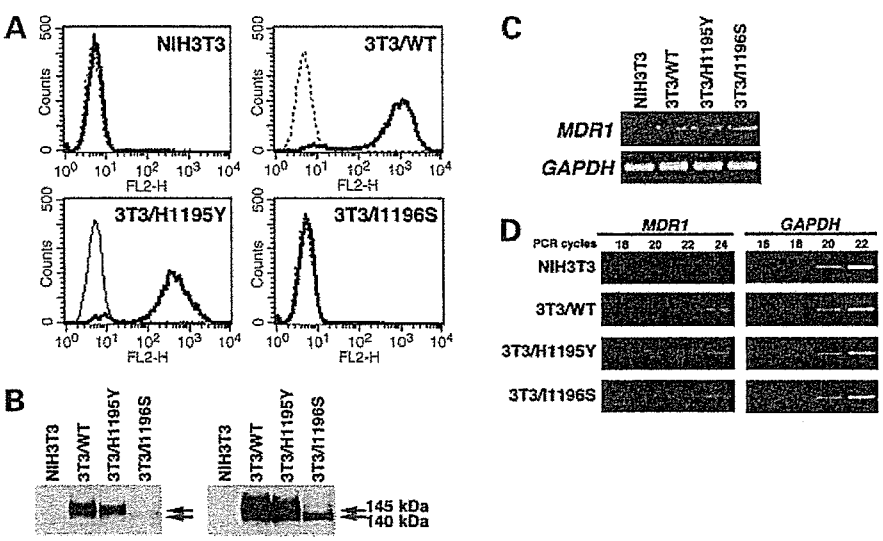

Figure 2. P-gp expression, *MDR1* cDNA integration, and *MDR1* mRNA expression in NIH3T3 transfectants. **A,** detection of cell surface expression of P-gp by FACS analysis. Parental NIH3T3 cells and the corresponding *MDR1* transfectants were harvested and then incubated with or without a biotinylated $F(ab')_2$ fragment of MRK16 followed by treatment with R-phycoerythrin-conjugated streptavidin. After washing, the fluorescence intensities were calculated using FACSCalibur. *Bold* and *dotted lines,* cells incubated with or without MRK16, respectively. **B,** Western blot analysis of P-gp in the *MDR1* transfectants. Protein extracts (20 μg) were subjected to Western immunoblotting analysis using the anti-P-gp monoclonal antibody C219 (1 μg/mL). *Left* and *right,* short (5 min) and long (15 min) exposures, respectively. **C,** genomic PCR analysis of exogenous *MDR1* cDNA in the *MDR1* transfectants. *MDR1* cDNA (3,561 bp) and *GAPDH* (551 bp) were amplified from genomic DNA preparations by PCR. *GAPDH* amplification was used as an internal control. **D,** reverse transcription-PCR analysis of *MDR1* transcripts in the NIH3T3 transfectants. *MDR1* (702 bp) and *GAPDH* (551 bp) transcripts were amplified by reverse transcription-PCR from 0.3 μg total RNA over the indicated number of cycles. *GAPDH* was again used as an internal control.

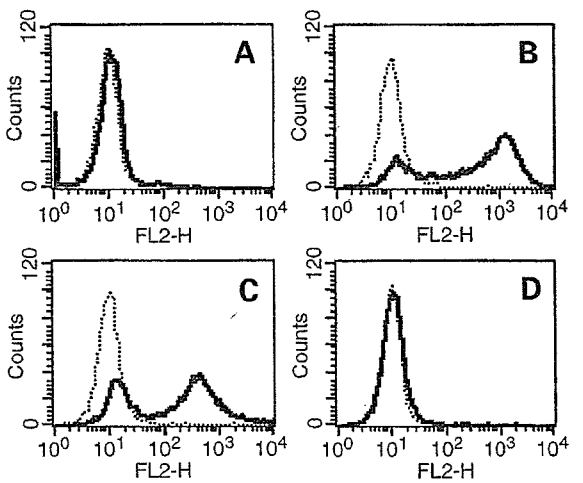

Figure 3. Cell surface expression of P-gp in retrovirally transduced cells. Cells were transduced with WT or mutant *MDR1* retroviruses, harvested, and incubated with or without a biotinylated $F(ab')_2$ fragment of MRK16 followed by treatment with R-phycoerythrin-conjugated streptavidin. After washing, the fluorescence intensities were calculated using FACSCalibur. *Bold* and *dotted lines,* cells incubated with or without MRK16, respectively. **A,** parental NIH3T3 cells. **B,** NIH3T3 cells transduced with WT *MDR1* retrovirus. **C,** NIH3T3 cells transduced with H1195Y *MDR1* retrovirus. **D,** NIH3T3 cells transduced with I1196S *MDR1* retrovirus.

in these cells and it is also significant that 3T3/I1196S cells showed no increased resistance to these chemotherapeutic agents when compared with the parental cells (Fig. 4), although I1196S P-gp was found to be expressed at low levels in 3T3/I1196S cells.

Loss of ATP-Binding Ability in I1196S P-gp

Because H1195Y P-gp and I1196S P-gp have amino acid substitutions in the second ATP-binding site of P-gp, we examined the ATP-binding activities of these variants. 3T3/I1196S clones were isolated and screened for higher P-gp expression, and clone 23 was found to contain the highest expression levels of I1196S P-gp. 3T3/I1196S clone 23 was thus used in these analyses (Fig. 5A). Because 3T3/I1196S clone 23 expressed ~25% of the WT P-gp levels, and 3T3/H1195Y cells expressed ~50% of the WT levels, we normalized these amounts in the relevant experiments (Fig. 5B and C). It was significant that the I1196S P-gp species showed no ATP-binding activity in either the absence or presence of 50 μmol/L verapamil (Fig. 5B and D). However, verapamil stimulated the nucleotide trapping of both WT P-gp and H1195Y P-gp, both of which showed similar levels of ATP-binding activity (Fig. 5C and D). These results suggest that I1196S P-gp lacks ATP-binding activity and therefore cannot function as an efflux pump.

Discussion

P-gp encoded by the *MDR1* gene is an important factor in the determination of the pharmacokinetics of its substrates, which include several anticancer drugs, as the coadministration of these agents and known P-gp inhibitors increases both the plasma concentration and the area under the concentration-time curve of these substrates (10, 11). C3435T *MDR1* was reported previously as a synonymous SNP that is associated with low intestinal P-gp expression, low P-gp activity, and high digoxin absorption (14). The association of a low level of P-gp activity was also observed with the *MDR1**2 haplotype containing C1236T *MDR1*, G2677T *MDR1*, and C3435T *MDR1* SNPs (17), but the details of the underlying mechanisms are still unknown. A *MDR1* SNP that causes a deficiency in P-gp function has not been reported previously.

In our previous and present studies, we have identified two nonsynonymous germ-line mutations, C3583T *MDR1* and T3587G *MDR1*. The C3583T *MDR1* substitutes a tyrosine for the His^{1195} residue of P-gp, whereas the T3587G *MDR1* results in a serine substitution for Ile^{1196}. Importantly, both of these residues are located in the Walker B region of the second ATP-binding site of P-gp (Fig. 1A). The Ile^{1196} residue in the P-gp is highly conserved among the members of ATP-binding cassette transporter superfamilies, but His^{1195} is not conserved among these proteins (refs. 22, 23; Fig. 1B). To examine the possible functional implications of these mutations, we established mutant *MDR1* cDNA transfectants and analyzed the biological consequences of the amino acid changes caused by these mutations.

Genetic variations have been known to affect mRNA expression and stability and also disrupt protein expression levels, turnover, and function. Because our study was designed to examine the possible effects of mutations in the coding region of the *MDR1* gene on protein expression levels, turnover, or function, we needed to establish WT or mutant *MDR1* transfectants that expressed similar amounts of *MDR1* mRNA. When standard two-promoter expression plasmid vectors are used for cDNA transfer, a high degree of variation in the expression of the transgene among transfectant clones may occur due to their different integration sites in the host genome and the possible effects of neighboring enhancers and/or silencers. We therefore

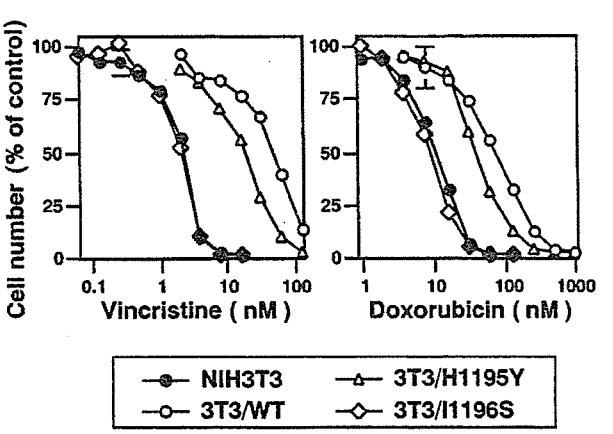

Figure 4. Drug resistance of the mutant *MDR1* transfectants. NIH3T3 (●), 3T3/WT (○), 3T3/H1195Y (△), and 3T3/I1196S (◇) cells were cultured for 5 d with various concentrations of vincristine or doxorubicin. Cell numbers were determined using a cell counter. *Points,* mean of triplicate experiments; *bars,* SD.

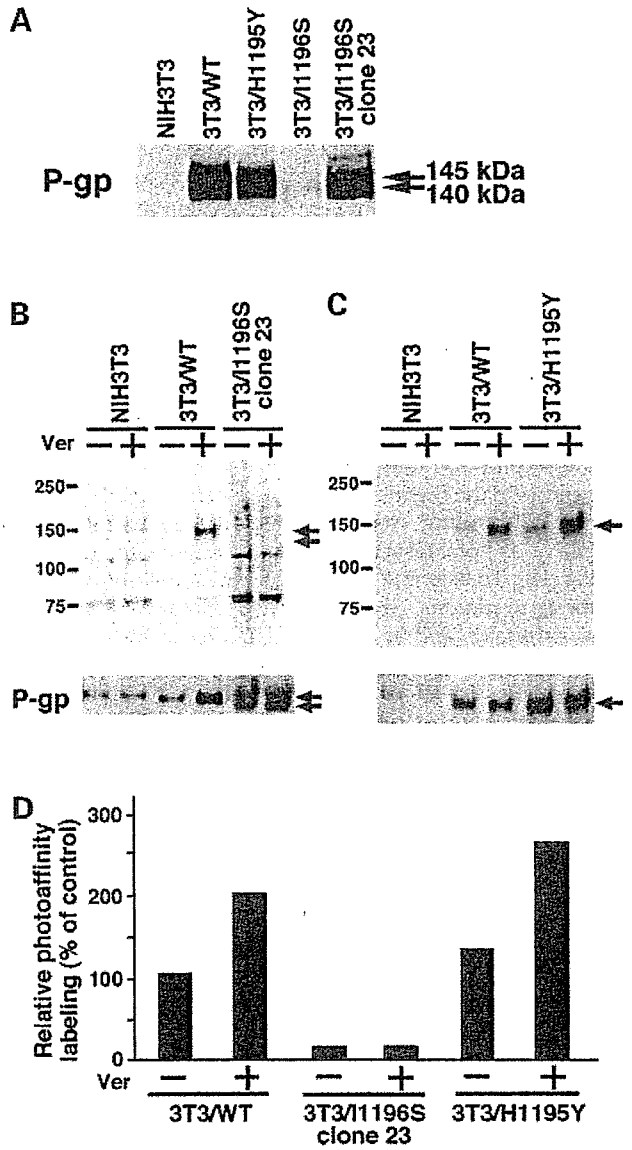

Figure 5. ATP-binding activities in the mutant *MDR1* transfectants. **A,** P-gp expression levels in the transfectants. Protein (20 μg) was loaded in each lane and subjected to Western blotting analysis using the anti-P-gp monoclonal antibody C219. **B,** ATP-binding activity of I1196S P-gp. Plasma membrane protein extracts of NIH3T3 (20 μg), 3T3/WT (5 μg), and 3T3/I1196S clone 23 (20 μg) cells were incubated with 10 μmol/L 8-azido-[α-^{32}P]ATP and 200 μmol/L vanadate in the absence (−) or presence (+) of 50 μmol/L verapamil for 10 min at 37°C. The proteins were then photoaffinity labeled by UV irradiation after the removal of unbound ligands and analyzed as described in Materials and Methods. *Top,* autoradiography using a radioimaging analyzer; *bottom,* Western blotting analysis of the same blot with the anti-P-gp antibody C219. *Arrows,* P-gps. **C,** ATP-binding activity of H1195Y P-gp. Plasma membrane protein extracts of NIH3T3 (20 μg), 3T3/WT (10 μg), and 3T3/H1195Y (20 μg) cells were analyzed as in **B.** *Top,* autoradiography using a radioimaging analyzer; *bottom,* Western blotting analysis of the same blot with the anti-P-gp antibody C219. *Arrows,* P-gps. **D,** relative ATP-binding activity of mutant P-gps. The trapped 8-azido-[α-^{32}P]ATP in the WT and mutant P-gps were quantified using BAS2500 imaging and normalized to the protein expression levels, and the relative photoaffinity labeling of each was then plotted. Two independent experiments were done, and the average of these analyses is shown.

used our previously reported flexible bicistronic vector system that uses an IRES to coexpress dominant drug-selectable markers, such as *dihydrofolate reductase* (*DHFR*) or *ZEO*, with the mutant *MDR1* gene (24, 25).

We reported previously the construction of bicistronic vectors in which the *MDR1* gene is coexpressed with herpes simplex virus-thymidine kinase (26–28), α-galactosidase A (28, 29), O^6-methylguanine DNA methyltransferase (30, 31), p47 of NADPH oxidase (32), and gp91 of NADPH oxidase (19, 33). We have further shown in this system that the drug treatments facilitated the enrichment or elimination of cells expressing the other nonselectable genes.

We next used this system to express mutant ATP-binding cassette transporters. We generated bicistronic pHa-BCRP-IRES-DHFR constructs to analyze the effects of *BCRP* coding SNPs on protein expression (34, 35). In the previous study, cells were transfected with pHa-BCRP-IRES-DHFR vectors containing either WT, G34A, C421A, or 944-949-deleted *BCRP* cDNA and then selected with methotrexate. In the resulting transfectants, a single mRNA is transcribed under control of a retrovirus long terminal repeat promoter, and two gene products are translated independently from a bicistronic mRNA. The upstream *BCRP* cDNA is translated cap-dependently, and the downstream *DHFR* cDNA is translated under a control of the IRES. Because only one mRNA species is transcribed, the cells expressing *DHFR* theoretically always coexpress the *BCRP* cDNA. We therefore combined all of the methotrexate-resistant colonies (>100) and used these mixed populations of methotrexate-resistant cells for further analysis. In this case, the expression of *BCRP* mRNA will reflect the mean levels for the transfectant clones and the mRNA levels within the mixed population will not be greatly affected by the expression levels of an individual clone. Indeed, we subsequently showed that four BCRP transfectants (mixed populations established after methotrexate selection) expressed similar levels of exogenous *BCRP* mRNA (34, 35). Additional FACS analysis then showed that almost all of the methotrexate-selected cells expressed BCRP on their cell surfaces. We then showed that BCRP expression from C421A *BCRP* cDNA is markedly lower than the WT.

In our present study, we constructed similar pCAL-MDR-IRES-ZEO bicistronic vectors that carry either WT or mutant *MDR1* cDNA insert. The transfectants were then selected with zeocin, and each of the resistant colonies (>100) were combined and used for further studies. As shown in Fig. 2A, most of the 3T3/WT and 3T3/H1195Y cells expressed cell surface P-gp. We also showed that the transfectants possess similar plasmid copy numbers (Fig. 2C) and similar levels of *MDR1* mRNA (Fig. 2D). To confirm our finding of a lower expression level of H1195Y P-gp, we did retrovirus-mediated gene transfer. Cells transduced with H1195Y *MDR1* retrovirus showed slightly lower P-gp expression levels than those transduced with WT *MDR1* retrovirus (Fig. 3). We therefore speculate that the difference in P-gp expression between 3T3/WT and 3T3/H1195Y cells is genuine and can be attributed to post-transcriptional events, such as protein maturation and/or stability.

Dubin-Johnson syndrome is an inherited disorder characterized by chronic conjugated hyperbilirubinemia due to the absence or dysfunction of the multidrug resistance-associated protein 2 (MRP2). Some Dubin-Johnson syndrome patients express mutant MRP2 proteins with amino acid substitutions or deletions (36–38). R768W MRP2, which has an amino acid substitution in signature C of the first ATP-binding site of the protein, is associated with relatively high serum bilirubin concentrations in affected patients (38) and this mutant protein is not properly glycosylated (36). Q1382R MRP2, a mutation that is located between the Walker A and the signature C regions of the second ATP-binding site, results in a lack of ATP hydrolysis activity (36). Moreover, the MRP2 mutant, which has a deletion in both its Arg^{1392} and Met^{1393} residues located between the Walker A and the signature C regions of the second ATP-binding site, is also a nonfunctional protein that shows impaired maturation and is sequestered in the endoplasmic reticulum (37). Hence, some MRP2 mutants that have mutations/deletions in the ATP-binding sites and lack ATP-hydrolyzing activity are underglycosylated, have not matured, and are unstable. We show in our current experiments that the I1196S P-gp also lacks ATP-binding activity and that its expression levels in 3T3/I1196S cells are markedly lower than in 3T3/WT cells. In addition, whereas the WT P-gp migrates as a 145-kDa protein, the I1196S P-gp migrates as a 140-kDa protein (Fig. 2B). The SDS-PAGE profile of I1196S P-gp is also very similar to the glycosylation-deficient P-gp that has the three amino acid substitutions, N91Q, N94Q, and N99Q (39). Taken together, these data suggest the possibility that I1196S P-gp does not undergo proper maturation, which results in low protein expression levels. Analyses of the biosynthesis and glycosylation status of I1196S P-gp are ongoing in our laboratory.

The conserved Asp^{1200} in the Walker B region of P-gp is required for the binding and hydrolysis of ATP (40, 41). Our present study also shows that substitution of serine for Ile^{1196} results in the loss of ATP-binding activity but that the substitution of tyrosine for His^{1195} does not affect P-gp function. It is not yet fully understood why mutant ATP-binding cassette transporters that lack ATP-binding activity are unstable, but defects in proper protein folding, particularly in ATP-binding sites, seem to be associated with protein degradation.

In our current study, we have also identified the T3587G and C3583T germ-line mutations in the *MDR1* gene in two individuals (0.3%) from a Japanese population of 605 individuals. In each case, however, these subjects were heterozygous for either the T3587G or C3583T allele. We contend, therefore, that there are two principal questions that arise from these findings: (*a*) the clinical significance of a homozygous T3587G *MDR1* genotype and (*b*) the clinical significance of a heterozygous T3587G *MDR1* genotype. Because the studies of *MDR1* double-knockout mice (*mdr1a/mdr1b*−/− mice) have shown that a *MDR1* deficiency causes large alterations in the pharmacokinetics of digoxin, vinblastine, and other drugs (12, 13), patients without P-gp function would also expected to show abnormal pharmacokinetics of P-gp substrate anticancer agents. Significantly, this may lead to potentially life-threatening side effects during cancer chemotherapy. Our present experiments have suggested the possible existence of a nonfunctional P-gp phenotype, but the extremely low allelic frequency of the T3587G *MDR1* mutation in our Japanese cohort makes it difficult to assess the relevance of a homozygous T3587G *MDR1* genotype in a clinical study. Hence, the existence of a subpopulation that has a high frequency of T3587G *MDR1* alleles would be necessary to detect homozygotes. It is likely that, in the absence of this, the prior genotype screening of homozygous T3587G *MDR1* patients undergoing cancer chemotherapy with P-gp substrate anticancer agents would be fruitless.

Another possible clinical study that could be undertaken would focus on T3587G *MDR1* heterozygous patients. We have identified heterozygous T3587G carriers in our Japanese population at a ratio of 1:300. In this regard, it is noteworthy that, in a previous report from our laboratory, a heterozygous T3587G *MDR1* patient treated with irinotecan showed the highest renal clearance of SN-38 among the group of irinotecan-treated patients in the study, although the renal clearances of irinotecan and SN-38 glucuronide in this individual were in the intermediate levels (17). However, it is not possible at this early stage to speculate on the effects of a heterozygous T3587G *MDR1* mutation from the results of only a single patient. To further clarify the consequences of a heterozygous T3587G allele, it will be necessary to further screen patients with T3587G *MDR1* mutation and examine whether they exhibit any aberrant kinetics or unusual toxicities as a result of treatments with *MDR1*-related anticancer agents. Such studies are currently ongoing in our laboratory and we wish to assess in the future whether the T3587G *MDR1* mutation would indeed be a candidate to be included in a putative SNP genotyping kit that would facilitate the screening of patients undergoing cancer therapy with P-gp substrates.

In a separate previous study from our laboratory, we identified the C376T *BCRP* SNP that encodes a Q126stop truncated BCRP (34, 35). The calculated frequency of homozygous C376T *BCRP* carriers was found to be 1.4 in 10,000, and we have not identified a homozygous carrier at this stage. Additionally, we have also reported that the C421A polymorphism in the *BCRP* gene, which substitutes lysine for the Gln^{141} residue of BCRP, is frequently observed in Japanese populations. Significantly, the Gln^{141} residue of BCRP lies between the Walker A and the signature C regions of its ATP-binding site. Moreover, Q141K BCRP-expressing cells show low levels of BCRP expression compared with WT BCRP-expressing cells (34, 35). This SNP may thus be important in the pharmacokinetics of irinotecan-related anticancer agents because cancer patients with the C421A allele show higher area under the concentration-time curve values after treatment with diflomotecan, an oral analogue of irinotecan, than patients harboring the WT allele (42). Hence, screening for SNPs that affect the expression of ATP-binding cassette and other transporters as well as drug-metabolizing enzymes are potentially very important for devising the appropriate treatments for cancer patients.

References

1. Riordan JR, Deuchars K, Kartner N, Alon N, Trent J, Ling V. Amplification of P-glycoprotein genes in multidrug-resistant mammalian cell lines. Nature 1985;316:817–9.

2. Chen CJ, Chin JE, Ueda K, et al. Internal duplication and homology with bacterial transport proteins in the *mdr1* (P-glycoprotein) gene from multidrug-resistant human cells. Cell 1986;47:381–9.

3. Shen DW, Fojo A, Chin JE, et al. Human multidrug-resistant cell lines: increased *mdr1* expression can precede gene amplification. Science 1986;232:643–5.

4. Gottesman MM, Hrycyna CA, Schoenlein PV, Germamm UA, Pastan I. Genetic analysis of the multidrug transporter. Annu Rev Genet 1995;29: 607–49.

5. Fojo AT, Ueda K, Slamon DJ, Poplack DG, Gottesman MM, Pastan I. Expression of a multidrug-resistance gene in human tumors and tissues. Proc Natl Acad Sci U S A 1987;84:265–9.

6. Cordon-Cardo C, O'Brien JP, Casals D, et al. Multidrug-resistance gene (P-glycoprotein) is expressed by endothelial cells at blood-brain barrier sites. Proc Natl Acad Sci U S A 1989;86:695–8.

7. Lown KS, Mayo RR, Leichtman AB, et al. Role of intestinal P-glycoprotein (mdr1) in interpatient variation in the oral bioavailability of cyclosporine. Clin Pharmacol Ther 1997;62:248–60.

8. van Asperen J, Schinkel AH, Beijnen JH, Nooijen WJ, Borst P, van Tellingen O. Altered pharmacokinetics of vinblastine in Mdr1a P-glycoprotein-deficient Mice. J Natl Cancer Inst 1996;17:994–9.

9. Hori R, Okamura N, Aiba T, Tanigawara Y. Role of P-glycoprotein in renal tubular secretion of digoxin in the isolated perfused rat kidney. J Pharmacol Exp Ther 1993;266:1620–5.

10. Merlin JL, Guerci A, Marchal S, et al. Comparative evaluation of S9788, verapamil, and cyclosporine A in K562 human leukemia cell lines and in P-glycoprotein-expressing samples from patients with hematologic malignancies. Blood 1994;84:262–9.

11. Mickisch GH, Kossig J, Keihauer G, Schlick E, Tschada RK, Alken PM. Effects of calcium antagonists in multidrug resistant primary human renal cell carcinomas. Cancer Res 1990;50:3670–4.

12. Schinkel AH, Wagenaar E, Mol CA, van Deemter L. P-glycoprotein in the blood-brain barrier of mice influences the brain penetration and pharmacological activity of many drugs. J Clin Invest 1996;97:2517–24.

13. Schinkel AH, Mayer U, Wagenaar E, et al. Normal viability and altered pharmacokinetics in mice lacking mdr1-type (drug-transporting) P-glycoproteins. Proc Natl Acad Sci U S A 1997;94:4028–33.

14. Hoffmeyer S, Burk O, von Richter O, et al. Functional polymorphism of the human multidrug resistance gene: multiple sequence variations and correlation of one allele with P-glycoprotein expression and activity *in vivo*. Proc Natl Acad Sci U S A 2000;97:3473–8.

15. Kurata Y, Ieiri I, Kimura M, et al. Role of human MDR1 gene polymorphism in bioavailability and interaction of digoxin, a substrate of P-glycoprotein. Clin Pharmacol Ther 2002;72:209–19.

16. Hitzl M, Drescher S, van der Kuip H, et al. The C3435T mutation in the human *MDR1* gene is associated with altered efflux of the P-glycoprotein substrate rhodamine 123 from $CD56^+$ natural killer cells. Pharmacogenetics 2001;11:293–8.

17. Sai K, Kaniwa N, Itoda M, et al. Haplotype analysis of *ABCB1/MDR1* blocks in a Japanese population reveals genotype-dependent renal clearance of irinotecan. Pharmacogenetics 2003;13:741–57.

18. Kiwaki K, Kanegae Y, Saito I, et al. Correction of ornithine transcarbamylase deficiency in adult spf(ash) mice and in OTC-deficient human hepatocytes with recombinant adenoviruses bearing the CAG promoter. Hum Gene Ther 1996;7:821–30.

19. Sugimoto Y, Tsukahara S, Sato S, et al. Drug-selected co-expression of P-glycoprotein and gp91 *in vivo* from an *MDR1*-bicistronic retrovirus vector Ha-MDR-IRES-gp91. J Gene Med 2003;5:366–76.

20. Kartner N, Evernden-Porelle D, Bradley G, Ling V. Detection of P-glycoprotein in multidrug-resistant cell lines by monoclonal antibodies. Nature 1985;316:820–3.

21. Takada Y, Yamada K, Taguchi Y, et al. Non-equivalent cooperation between the two nucleotide-binding folds of P-glycoprotein. Biochim Biophys Acta 1998;1373:131–6.

22. Payen LF, Gao M, Westlake CJ, Cole SPC, Deeley RG. Role of carboxylate residues adjacent to the conserved core Walker B motifs in the catalytic cycle of multidrug resistance protein 1 (ABCC1). J Biol Chem 2003;278:38537–47.

23. Ryu S, Kawage T, Nada S, Yamagichi A. Identification of basic residues involved in drug export function of human multidrug resistance-associated protein 2. J Biol Chem 2000;275:39617–24.

24. Sugimoto Y, Aksentijevich I, Gottesman MM, Pastan I. Efficient expression of drug-selectable genes in retroviral vectors under control of an internal ribosome entry site. Biotechnology 1994;12:694–8.

25. Zhang S, Sugimoto Y, Shoshani T, Pastan I, Gottesman MM. A pHaMDR-DHFR bicistronic expression system for mutation analysis of P-glycoprotein. Methods Enzymol 1998;292:474–80.

26. Sugimoto Y, Hrycyna C, Aksentijevich I, Pastan I, Gottesman MM. Co-expression of a multidrug resistahce gene (*MDR1*) and herpes simplex virus thymidine kinase gene as part of a bicistronic mRNA in a retrovirus vector allows selective killing of *MDR1*-transduced cells. Clin Cancer Res 1995;1:447–57.

27. Sugimoto Y, Sato S, Tsukahara S, et al. Coexpression of a multidrug resiatance gene (MDR1) and herpes simplex virus thymidine kinase gene in a bicistronic retroviral vector Ha-MDR-IRES-TK allows selective killing of *MDR1*-transduced human tumors transplanted in nude mice. Cancer Gene Ther 1997;4:51–8.

28. Sugimoto Y, Gottesman MM, Pastan I, Tsuruo T. Construction of *MDR1* vectors for gene therapy. Methods Enzymol 1998;292:523–37.

29. Sugimoto Y, Aksentijevich I, Murray GJ, Brady RO, Pastan I, Gottesman MM. Retroviral coexpression of a multidrug resistance gene (*MDR1*) and human α-galactosidase A for gene therapy of Fabry disease. Hum Gene Ther 1995;6:905–15.

30. Suzuki M, Sugimoto Y, Tsukahara S, Okochi E, Gottesman MM, Tsuruo T. Retroviral co-expression of two different types of drug-resistant genes to protect normal cells from combination chemotherapy. Clin Cancer Res 1997;3:947–54.

31. Suzuki M, Sugimoto Y, Tsuruo T. Efficient protection of cells from the genotoxicity of nitrosoureas by the retrovirus-mediated transfer of human O^6-methylguanine-DNA methyltransferase using bicistronic vectors with human multidrug resistance gene 1. Mutat Res 1998;410:133–41.

32. Iwata M, Nunoi H, Matsuda I, Kanegasaki S, Tsuruo T, Sugimoto Y. Drug-selected complete restoration of superoxide generation in Epstein-Barr virus-transformed B cells from p47phox-deficient chronic granulomatous disease patients using a bicistronic retrovirus vector encoding a human multidrug resistance gene (*MDR1*) and the *p47phox* gene. Hum Genet 1998;103:419–23.

33. Sokolic RA, Sekhsaria S, Sugimoto Y, et al. A bicistronic retrovirus vector containing a picornavirus internal ribosome entry site allows for correction of X-linked CGD by selection for *MDR1* expression. Blood 1996;87:42–50.

34. Imai Y, Nakane M, Kage K, et al. C421A polymorphism in the human breast cancer resistance protein gene is associated with low expression of Q141K protein and low-level drug resistance. Mol Cancer Ther 2002;1: 611–6.

35. Sugimoto Y, Tsukahara S, Ishikawa E, Mitsuhashi J. Breast cancer resistance protein: molecular target for anticancer drug resistance and pharmacokinetics/pharmacodynamics. Cancer Sci 2005;96:457–65.

36. Hashimoto K, Uchiumi T, Konno T, et al. Trafficking and functional defects by mutations of the ATP-binding domains in MRP2 in patients with Dubin-Johnson syndrome. Hepatology 2002;36:1236–45.

37. Keitel V, Kartenberk J, Nies AT, Spring H, Brom M, Keppler D. Impaired protein maturation of the conjugate export pump multidrug resistance protein 2 as a consequence of a deletion mutation in Dubin-Johnson syndrome. Hepatology 2000;32:1317–28.

38. Wada M, Toh S, Taniguchi K, et al. Mutations in the canalicular multispecific organic anion transporter (*cMOAT*) gene, a novel ABC transporter, in patients with hyperbilirubinemia II/Dubin-Johnson syndrome. Hum Mol Genet 1998;7:203–7.

39. Gribar JJ, Ramachandra M, Hrycyna CA, Dey S, Ambudkar SV. Functional characterization of glycosylation-deficient human P-glycoprotein using a vaccinia virus expression system. J Membr Biol 2000; 173:203–14.

40. Hrycyna CA, Ramachandra M, Germann UA, Cheng PW, Pastan L, Gottesman MM. Both ATP sites of human P-glycoprotein are essential but not symmetric. Biochemistry 1999;38:13887–99.

41. Urbatsch IL, Beaudet L, Carrier I, Gros P. Mutations in either nucleotide-binding site of P-glycoprotein (Mdr3) prevent vanadate trapping of nucleotide at both sites. Biochemistry 1998;37:4592–602.

42. Sparredoom A, Gelderblom H, Marsh S, et al. Diflomotecan pharmacokinetics in relation to ABCG2 421C>A genotype. Clin Pharmacol Ther 2004;76:38–44.

FEBS Letters 580 (2006) 4371–4376

Platelet derived growth factor regulates ABCA1 expression in vascular smooth muscle cells

Sachi Nagao[a], Koji Murao[a,*], Hitomi Imachi[a], Wen-Ming Cao[a], Xiao Yu[a], Junhua Li[a], Kensuke Matsumoto[a], Takamasa Nishiuchi[a], Rania A.M. Ahmed[a], Norman C.W. Wong[b], Kazumitsu Ueda[c], Toshihiko Ishida[a]

[a] *Division of Endocrinology and Metabolism, Department of Internal Medicine, Faculty of Medicine, Kagawa University, 1750-1 Ikenobe Miki-CHO, Kita-gun, Kagawa, Japan*

[b] *Departments of Medicine and Biochemistry & Molecular Biology, Faculty of Medicine, University of Calgary, Health Sciences Center, 3330 Hospital Drive NW, Calgary, Alta., Canada T2N 4N1*

[c] *Laboratory of Cellular Biochemistry, Division of Applied Life Sciences, Graduate School of Agriculture, Kyoto University, Kyoto 606-8502, Japan*

Received 10 May 2006; revised 20 June 2006; accepted 2 July 2006

Available online 10 July 2006

Edited by Laszlo Nagy

Abstract The ATP-binding cassette transporter A1 (ABCA1) regulates lipid efflux from peripheral cells to High-density lipoprotein. The platelet-derived growth factor (PDGF) is a potent mitogen that enables vascular smooth muscle cells to participate in atherosclerosis. In this report, we showed that PDGF suppressed endogenous expression of ABCA1 in cultured vascular smooth muscle cells. Exposure of CRL-208 cells to PDGF elicited a rapid phosphorylation of a kinase downstream from PI3-K, Akt. The constitutively active form of both p110, a subunit of PI3-K, and Akt inhibited activity of the ABCA1 promoter. In conclusion, PI3-K-Akt pathways participate in PDGF-suppression of ABCA1 expression.

Keywords: Platelet-derived growth factor; ATP-binding cassette transporter A1; Smooth muscle cell; Protein kinase B

1. Introduction

Atherosclerotic coronary artery disease (CAD) is a major public heath burden in developed countries. High-density lipoprotein (HDL) plays a critical role in cholesterol metabolism because they mediate a normal physiologic process, the so-called reverse cholesterol transport (RCT) [1,2]. In this process HDL particles shuttle cholesterol from extra-hepatic tissues to the liver for further metabolism and excretion [1]. The ATP-binding cassette transporter A1 (ABCA1), a 254-kDa membrane protein, is a pivotal regulator of lipid efflux from cells to apolipoproteins [3]. ABCA1 plays an important role in RCT because mutations of this gene found in patients with Tangier disease cause impaired efflux of lipids to apolipoprotein A–I [3].

Abnormal proliferation of vascular smooth muscle cells (VSMCs) is a critical component of atherosclerosis and arterial restenosis after angioplasty [4]. The mechanism is believed to be related to a response to injury in which growth factors such as a platelet derived growth factor (PDGF) are released, thus stimulating proliferation and migration of VSMCs to the site resulting in the formation of a neointima. PDGF bound to its receptor leads to the activation of several cell-signaling pathways associated with both VSMC proliferation and migration, such as those related to mitogen-activated protein kinase (MAPK), extracellular signal-regulated kinase (ERK) 1/2, phospholipase C-γ (PLC-γ), and phosphatidylinositol 3-kinase (PI3-k) [5]. Protein kinase B (Akt) activation is dependent on the upstream kinase PI3-K and influences cellular functions by activation of various downstream effectors [6].

In the present study, the results of our studies suggest that PDGF acts via the PI3-K/Akt signal transduction pathway to suppress ABCA1 gene transcription.

2. Materials and methods

2.1. Material

LY294002, PD98059, Bisindolylmaleimide I were purchased from Calbiochem (La Jolla, CA). Recombinant rat PDGF-BB was purchased from R&D, Co. Ltd (CA). Antibody: Anti-ABCA1 monoclonal antibody KM3110 was generated against the C-terminal 20 amino acids of ABCA1 in mice. Apolipoprotein A–I (apoA–I) and acetylated LDL (AcLDL) were purchased from Funakoshi (Osaka, Japan).

2.2. Plasmid preparation

An expression vector encoding a constitutively active Akt (Akt-CA) and a dominant-negative mutant of Akt (Akt-DN) was described previously [7]. An expression vector encoding a constitutively active p110 subunit was gift from J. Downward (Imperial Cancer research Foundation, London, UK). An expression vector encoding a PTEN (phosphatase and tensin homologue deleted on chromosome ten) was a gift from J.E. Dixon (Univ. of Michigan, Arbor, MI).

Cell culture: Primary cultured human vascular smooth muscle cell was purchased (Applied Cell Biology Research, Kirkland, WA). Rat vascular smooth muscle cell line, CRL-2018 (obtained from ATCC, Manassas, VA) was grown in DMEM (Life Technologies, Tokyo, Japan) supplemented with 10% FCS.

2.3. Western blot analysis

The proteins were resuspended under reducing conditions and a 15 μg was fractionated by size on 7.5% SDS–polyacrylamide gels [8]. The membranes were blocked overnight at room temperature with 0.1% Tween 20 in PBS (PBS-T) containing anti-ABCA1 antibody KM3110 (diluted 1:5000 from whole antiserum). These membranes

*Corresponding author. Fax: +81 878 91 2147.
E-mail address: mkoji@kms.ac.jp (K. Murao).

0014-5793/$32.00
doi:10.1016/j.febslet.2006.07.001

were washed with PBS-T, incubated for 1 h at room temperature in PBS-T containing horseradish peroxidase-linked anti-mouse IgG (diluted 1/3000), rinsed in PBS-T.

2.4. Transfection of CRL-2018 cells and luciferase reporter gene assay

The reporter construct contained the ABCA1 gene sequence spanning the region from −919 to +224 as determined from the published sequence [8]. The segment of interest was amplified using PCR and cloned into the luciferase reporter gene (pABCA1-LUC). Purified reporter plasmid was transfected into CRL-2018 cells using a conventional cationic liposome transfection method (Lipofectamine, Life Technologies, Gaithersburg, MD). All assays were corrected for β-galactosidase activity and total amount of protein in each reaction was identical as previously described [9].

2.5. Immunoblotting of Akt

Akt phosphorylated at Ser473 or Thr308 was detected using a phospho-specific Akt polyclonal antibody and total Akt was detected by using phosphorylation-independent antibodies (Upstate biotechnology, NY) as described previously [10]. The protein bands were visualized by chemiluminescence.

2.6. Cholesterol efflux assay

The cells were labeled with ^{3}H-cholesterol (5 μCi/ml) incorporated into acetylated LDL (AcLDL) (30 μg AcLDL/ml). Cells underwent an equilibration step in media plus 2 mg/ml bovine serum albumin (BSA) for 12 h prior to efflux. After the equilibration period, cells were incubated with apoA–I (30 μg/ml) in DMEM/BSA for 5 h. ^{3}H-cholesterol efflux was expressed as medium [^{3}H] cholesterol radioactivity as a percentage of total [^{3}H] cholesterol radioactivity [11].

2.7. Statistical analysis

Statistical comparisons were made possible through the use of one-way analysis of variance and Student's *t*-test, with $P < 0.05$ considered significant.

3. Results

3.1. PDGF decreases ABCA1 expression in CRL-2018 cells

To test whether PDGF affected ABCA1 expression, we used Western blot analysis to measure the levels of endogenous ABCA1 expression in both primary cultured human smooth muscle cell and cell line, CRL-2018. Exposure of the cells to PDGF for 24 h decreased the abundance of endogenous ABCA1 protein as compared with that in cells maintained in control media (Fig. 1A and B).

3.2. Effect of PDGF on ABCA1 promoter activity

Next we measured transcriptional activity of the ABCA1 promoter in the CRL-2018 cells. CRL-208 cells transfected with pABCA1-LUC were exposed to varying concentrations of PDGF (Fig. 2A). Consistent with the observed changes in the levels of ABCA1 protein and mRNA, PDGF inhibited activity of the promoter in a dose dependent fashion with near maximum inhibition using 10 ng/ml of PDGF. To test whether protein kinases were involved in the inhibitory actions of PDGF on ABCA1 promoter activity, we studied the effect of pharmacological inhibitors on ABCA1 promoter activity. Therefore, exposure of the pABCA1-LUC transfected CRL-2018 cells to PDGF (10 ng/ml) was tested in the presence of inhibitors such as PI3-K (10 μM LY294002), a mitogen-activated ERK (10 μM PD98059), or PKC (Bisindolylmaleimide I) to the CRL-2018 cells. Results (Fig. 2B) showed that the inhibitory effect of PDGF on ABCA1 promoter activity was not sensitive to inhibitors of ERK or PKC but it was sensitive to LY294002, an inhibitor of PI3-K.

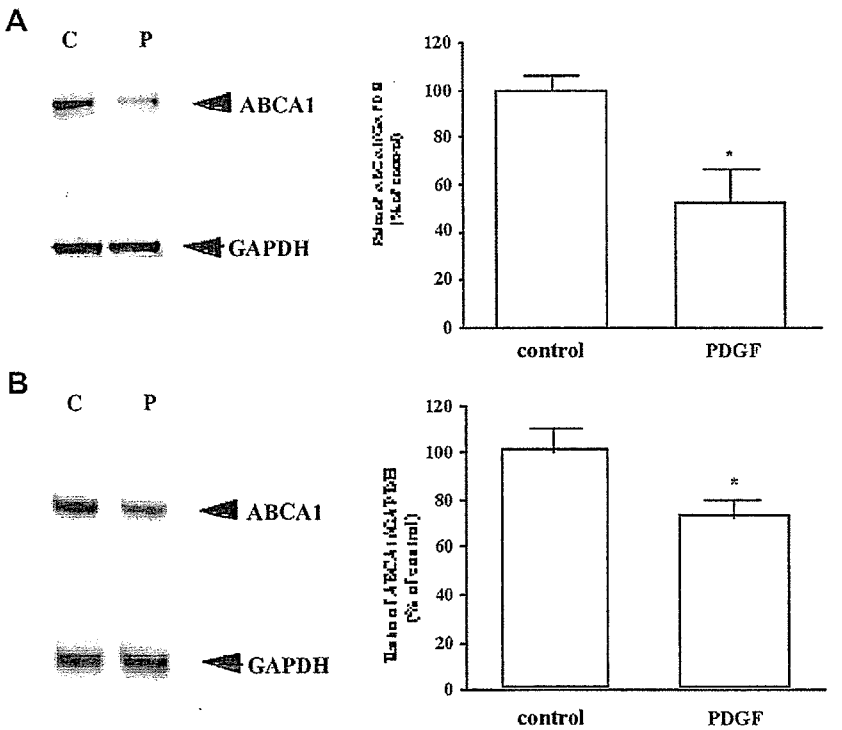

Fig. 1. Effect of PDGF on ABCA1 expression in CRL-2018 cells. (A,B) PDGF decreases ABCA1 protein expression. Human vascular smooth muscle cells (A) or CRL-2018 cells (B) were exposed to PDGF for 24 h and ABCA1 protein in total cell lysate was detected using Western blot analysis probed with an anti-ABCA1 antibody. (C) No-treatment or p: 10 ng/ml PDGF. A graph showing the mean ± S.E.M. of three experiments for each treatment group is shown on the right. The asterisk denotes a significant difference ($P < 0.01$).

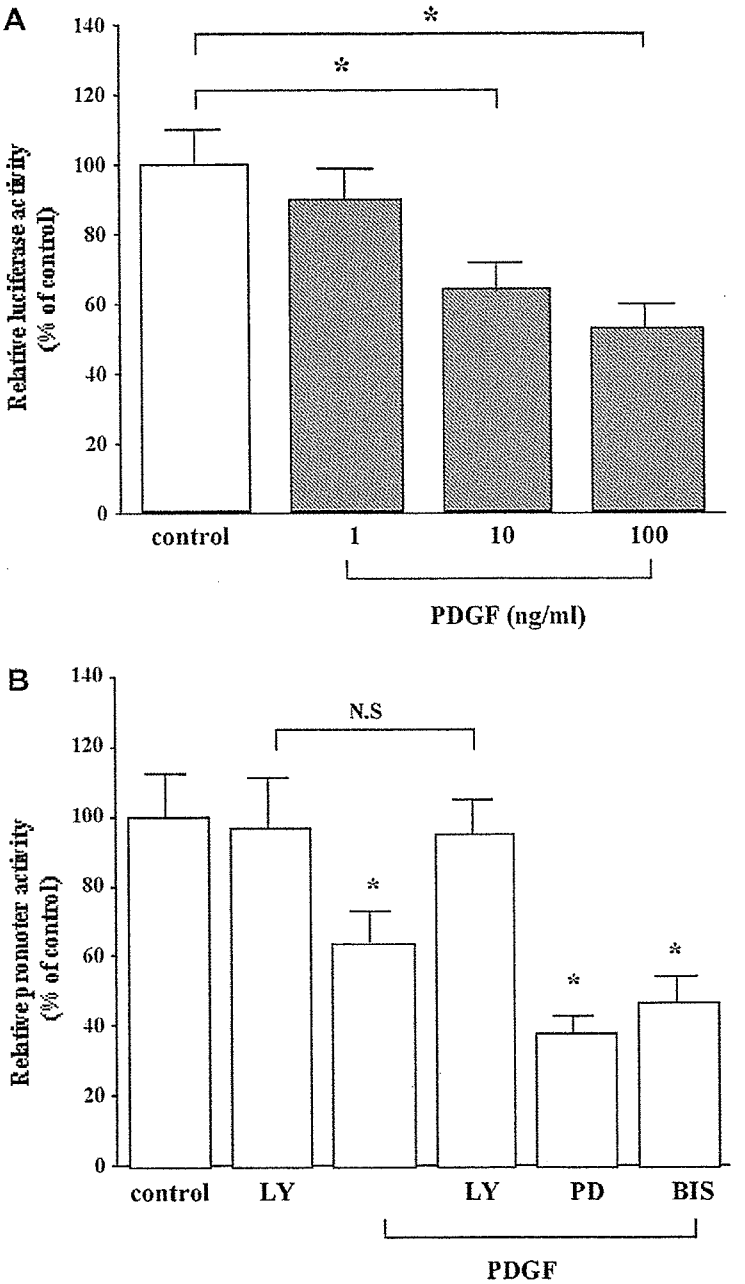

Fig. 2. Effect of PDGF on ABCA1 transcriptional activity and in CRL-2018 cells. (A) PDGF decreases ABCA1 gene transcription. CRL-2018 cells were transfected with pABCA1-LUC and treated with various concentration of PDGF for 24 h. Each data point shows the means ± S.E.M. of four separate transfections that were performed on separate days. The asterisk denotes a significant ($P < 0.01$). (B) A PI3-K inhibitor blocks the actions of PDGF. Effects of a PI3-K inhibitor LY294002 (LY), a MEK1 inhibitor PD98059 (PD), or a protein kinase C inhibitor Bisindolylmaleimide I (BIS) on PDGF (10 ng/ml)-inhibited ABCA1 transcriptional activity. Values represent the mean of triplicate determinations. The asterisk denotes a significant difference ($P < 0.01$).

3.3. Effect of PDGF on cholesterol efflux in CRL-2018 cells

To further demonstrate the inhibitory actions of PDGF, we took advantage of the fact that ABCA1 functions to facilitate cellular lipid efflux to HDL in the presence of ApoA–I [12]. This parameter was assessed by measuring cholesterol efflux from CRL-2018 cells to ApoA–I using ^{3}H-cholesterol delivered to the cells via acetylated-LDL uptake. We noted that pretreatment with PDGF (10 ng/ml) for 24 h proved to be most effective and therefore, all subsequent experiments were performed under these conditions. PDGF inhibited cholesterol efflux to 75% of control untreated cells (Fig. 3). As predicted from the preceding studies, LY294002 blocked PDGF-suppression of the cholesterol efflux but the PI3-K inhibitor had no stimulatory effect on basal efflux in the absence of PDGF.

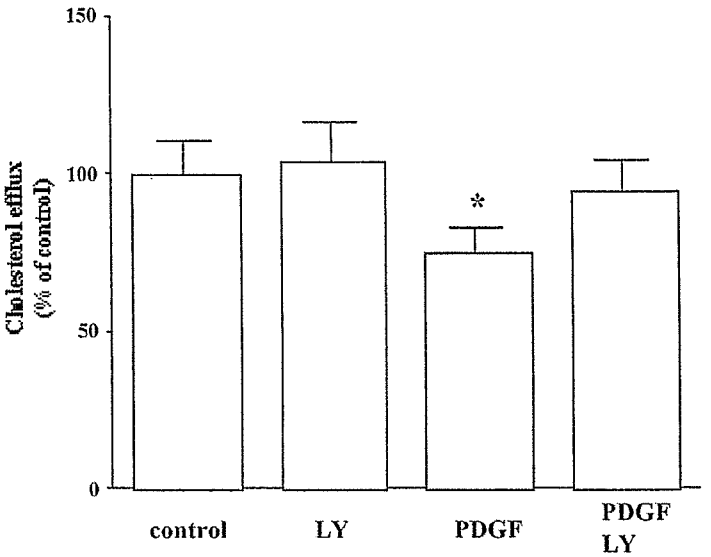

Fig. 3. PDGF inhibits cholesterol efflux in CRL-2018 cells. CRL-2018 cells were treated with PDGF (10 ng/ml), LY294002 (LY), or both PDGF and the inhibitor. The cells were incubated with apoA–I (50 μg/ml) in DMEM/BSA for 5 h. ApoA–I specific [^{3}H] cholesterol efflux was calculated and apoA–I-specific efflux in the absence of any treatment was normalized to 100%. Each individual experiment was performed in quadruplicate and the values show the mean ± S.E.M. The asterisk denotes a significant difference ($P < 0.01$). Lane 1; control, lane2; LY294002 (LY), lane 3; PDGF, lane 4; PDGF and LY294002 (LY).

3.4. Time course of Akt phosphorylation by PDGF

The preceding studies showed that PI3-kinase likely participated in the inhibitory effects of PDGF on ABCA1 expression. Since Akt is a potential target of the PI3-K, we wondered whether the use of PDGF could also activate Akt. To answer this question, we examined the kinetics of Akt activation by measuring phosphorylation of the residues Thr308 and Ser473. These sites are modified as a prerequisite for catalytic activity of Akt. The results (Fig. 4) showed that Akt phosphorylation was evident within 15 min following exposure of the CRL-2018 cells to PDGF and this activity reached a peak at 60 min.

3.5. Akt regulates ABCA1 promoter activity

Since Akt phosphorylation may participate in PDGF inhibition of ABCA1 expression, we asked whether Akt affected ABCA1 promoter activity. If so, then the actions of constitutively active Akt, p110 (a subunit of PI3-K), and PTEN (a natural inhibitor of PI3-K pathway) should affect activity of the promoter. As predicted, the results (Fig. 5A) showed that constitutively active Akt and p110 suppressed ABCA1 promoter activity in CRL-2018 cells. In contrast, the co-transfection of PTEN expression vector activated pABCA1-LUC activity.

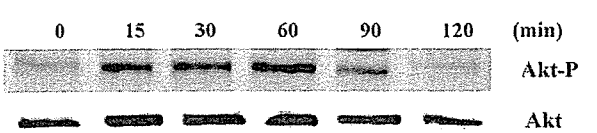

Fig. 4. PDGF stimulates the phosphorylation of Akt. CRL-2018 cells were exposed to 10 ng/ml PDGF for 0, 15, 30, 60, 90 and 120 min. Abundance of phosphorylated Akt was detected by Western blot analysis using a phospho-specific Akt antibody (Akt-P, upper portion). To show equal loading of protein in the each lane, the same blot was probed a second time with an Akt-specific antibody.

To further confirm the role of Akt, we tested the effects of a dominant negative mutant of Akt (Akt-DN) on ABCA1 promoter activity (Fig. 5B). Consistent with the above studies; PDGF inhibited the activity of the ABCA1 promoter and the expression of Akt-DN inhibited the actions of PDGF on ABCA1 promoter activity.

4. Discussion

In this report, we have summarized the results of studies showing that PDGF affected ABCA1 gene expression. To connect the actions of Akt with ABCA1 expression, we assessed the effects of both a constitutively active and a dominant negative form of Akt on ABCA1 promoter activity (Fig. 5). In agreement with our hypothesis, constitutively activated Akt mimiced the inhibitory action of PDGF on ABCA1 promoter activity and the dominant negative mutant blocked this effect. Further studies of the role of Akt in PDGF-mediated ABCA1 inhibition will be necessary to define the pathway by which PDGF affects the gene.

Since Akt/PKB is one of the downstream components of intracellular signaling triggered by PDGF, it is not surprising that Akt/PKB was phosphorylated following treatment of CRL-2018 cells with PDGF. Akt/PKB phosphorylation is negatively regulated by PTEN/MMAC1/TEP1 a tumor suppressor gene product. This protein is a phosphatase that dephosphorylates the 3′ position to reverse the reactions catalyzed by PI3-K [13]. Results in Fig. 5A showed that overexpression of PTEN increased ABCA1 promoter activity.

Many studies indicate that phenotypic modulation of SMC within atherosclerotic lesions is very complex and likely to involve many factors including growth factors and cytokines, inflammatory cell mediators, lipids, lipid peroxidation products, and reactive oxygen species [14,15]. Platelet-derived

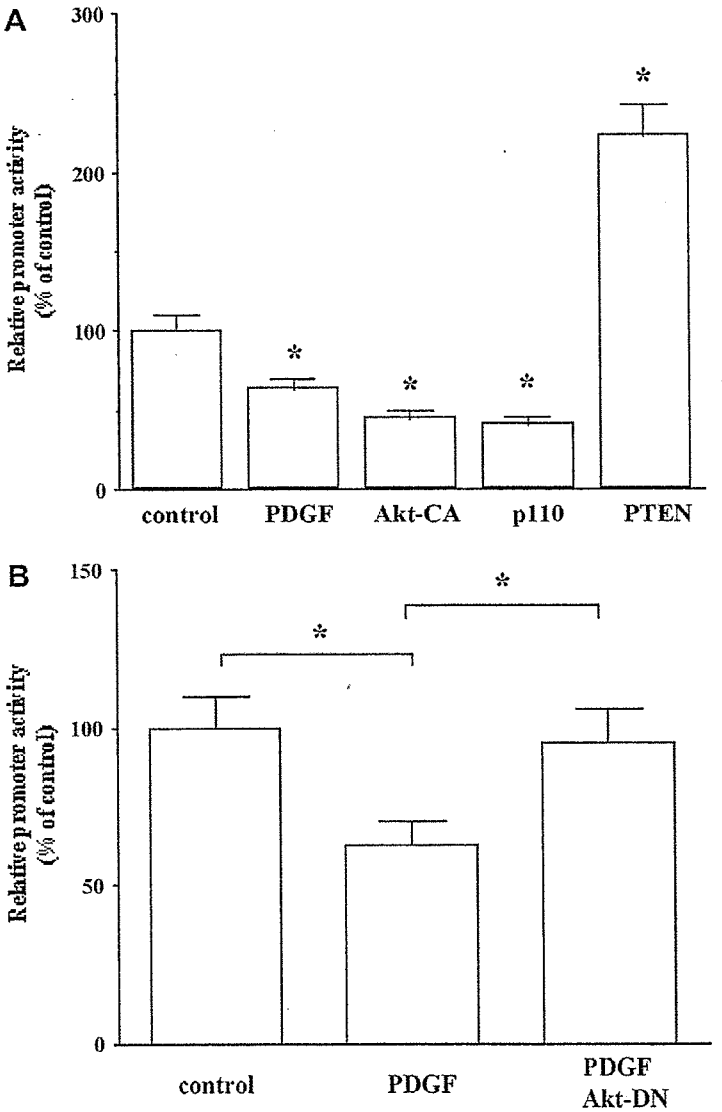

Fig. 5. Role of PI3-K/Akt signal transduction pathway on ABCA1 promoter activity by PDGF. (A) Effects of PI3-K components on ABCA1 promoter activity. CRL-2018 cells were transfected with pABCA1-LUC and empty vector (Cont), empty vector plus PDGF-treatment (PDGF), Akt-CA expression vector (Akt-CA), p110 expression vector (p110), and PTEN expression vector (PTEN). Each data point shows the means ± S.E.M. of four separate transfections that were performed on separate days. The asterisk denotes a significant difference ($P < 0.01$). (B) Dominant negative Akt blocks PDGF inhibition of ABCA1 transcription. CRL-2018 cells were transfected with pABCA1-LUC and empty vector or Akt-DN and then treated with PDGF. Each data point shows the means ± S.E.M. of four separate transfections that were performed on separate days. The asterisk denotes a significant difference ($P < 0.01$).

growth factor (PDGF) is a potent mitogen and chemoattractant that functions as an important mediator in the pathogenesis of vascular disease [16]. Our studies showed that inhibition of PI3-K completely blocked the effect of PDGF-suppressed ABCA1 promoter activity in VSMCs, whereas MEK1 and PKC inhibitors had no effect on this action, the PI3-K inhibitor LY294002 prevented the suppressive effects of PDGF. Although those pharmacological probes are relatively selective, we also verified the results by using the constitutively active form of p110, the subunit of PI3-K and PTEN, the natural inhibitor of PI3-K pathway. The concordance between the data using pharmacological probes and the constitutively active constructs provides evidence that ABCA1 gene expression is regulated by a PI3-K-dependent pathway. FoxO transcription factors have been implicated in regulating diverse cellular functions including differentiation, metabolism, proliferation, and survival. Furthermore, it is well acknowledged that Akt mediates many of the effect of growth factors downstream of PI3-K, and several FoxO proteins are now established substrates of Akt in this pathway [17]. We identified a putative FoxO response sequence on ABCA1 promoter by searching the BLASTN program in a genomic database. Further studies will be needed to determine the detailed mechanisms involved in the regulation of the ABCA1 gene.

In summary, the results in this report show that PDGF inhibits the expression of the endogenous ABCA1 in rat

vascular smooth muscle cell line, CRL-2018. This inhibitory effect of PDGF on ABCA1 promoter is mediated by PI3-K/Akt signal transduction pathway. These findings raise the possibility that PDGF may affect RTC by controlling ABCA1 expression.

References

[1] Fielding, C.J. and Fielding, P.E. (1995) Molecular physiology of reverse cholesterol transport. J. Lipid. Res. 36, 211–228.

[2] Tall, A.R. (1990) Plasma high density lipoproteins. Metabolism and relationship to atherogenesis. J. Clin. Invest. 86, 379–384.

[3] Tall, A.R. and Wang, N. (2000) Tangier disease as a test of the reverse cholesterol transport hypothesis. J. Clin. Invest. 106, 1205–1207.

[4] Newby, A.C. and Zaltsman, A.B. (2000) Molecular mechanisms in intimal hyperplasia. J. Pathol. 190, 300–309.

[5] Homma, Y., Sakamoto, H., Tsunoda, M., Aoki, M., Takenawa, T. and Ooyama, T. (1993) Evidence for involvement of phospholipase C-gamma 2 in signal transduction of platelet-derived growth factor in vascular smooth-muscle cells. Biochem. J. 290, 649–653.

[6] Shiojima, I. and Walsh, K. (2002) Role of Akt signaling in vascular homeostasis and angiogenesis. Circ. Res. 90, 1243–1250.

[7] Cao, W.M., Murao, K., Imachi, H., Sato, M., Nakano, T., Kodama, T., Sasaguri, Y., Wong, N.C., Takahara, J. and Ishida, T. (2001) Phosphatidylinositol 3-OH kinase-Akt/protein kinase B pathway mediates Gas6 induction of scavenger receptor a in immortalized human vascular smooth muscle cell line. Arterioscler. Thromb. Vasc. Biol. 21, 1592–1597.

[8] Langmann, T., Porsch-Ozcurumez, M., Heimerl, S., Probst, M., Moehle, C., Taher, M., Borsukova, H., Kielar, D., Kaminski, W.E., Dittrich-Wengenroth, E. and Schmitz, G. (2002) Identification of sterol-independent regulatory elements in the human ATP-binding cassette transporter A1 promoter: role of Sp1/3, E-box binding factors, and an oncostatin M-responsive element. J. Biol. Chem. 277, 14443–14450.

[9] Murao, K., Wada, Y., Nakamura, T., Taylor, A.H., Mooradian, A.D. and Wong, N.C. (1998) Effects of glucose and insulin on rat apolipoprotein A–I gene expression. J. Biol. Chem. 273, 18959–18965.

[10] Cao, W.M., Murao, K., Imachi, H., Yu, X., Dobashi, H., Yoshida, K., Muraoka, K., Kotsuna, N., Nagao, S., Wong, N.C. and Ishida, T. (2004) Insulin-like growth factor-I regulation of hepatic scavenger receptor class BI. Endocrinology 145, 5540–5547.

[11] Kiss, R.S., McManus, D.C., Franklin, V., Tan, W.L., McKenzie, A., Chimini, G. and Marcel, Y.L. (2003) The lipidation by hepatocytes of human apolipoprotein A–I occurs by both ABCA1-dependent and -independent pathways. J. Biol. Chem. 278, 10119–10127.

[12] Singaraja, R.R., Brunham, L.R., Visscher, H., Kastelein, J.J. and Hayden, M.R. (2003) Efflux and atherosclerosis: the clinical and biochemical impact of variations in the ABCA1 gene. Arterioscler. Thromb. Vasc. Biol. 23, 1322–1332.

[13] Maehama, T. and Dixon, J.E. (1998) The tumor suppressor, PTEN/MMAC1, dephosphorylates the lipid second messenger, phosphatidylinositol 3,4,5-trisphosphate. J. Biol. Chem. 273, 13375–13378.

[14] Lusis, A.J. (2000) Atherosclerosis. Nature 407, 233–241.

[15] Ross, R. (1999) Atherosclerosis – an inflammatory disease. N. Engl. J. Med. 340, 115–126.

[16] Seewald, S., Sachinidis, A., Seul, C., Kettenhofen, R., Ko, Y. and Vetter, H. (1997) The role of platelet-derived growth factor-BB-induced increase in cytosolic free Ca2+ in activation of mitogen-activated protein kinase and DNA synthesis in vascular smooth muscle cells. J. Hypertens. 15, 1671–1675.

[17] Accili, D. and Arden, K.C. (2004) FoxOs at the crossroads of cellular metabolism, differentiation, and transformation. Cell 117, 421–426.